People's Democratic Republic of Algeria
Ministry of Higher Education and Scientific Research

University M'Hamed BOUGARA – Boumerdes

Institute of Electrical and Electronic Engineering

Department of Power and Control Engineering

Final Year Project Report Presented in Partial Fulfilment of
the Requirements for the Degree of

MASTER

Option: **Power Engineering and Control Engineering**

Title:

Voltage Oriented and Model Predictive Control of Three-phase Vienna Rectifier

Presented by:

Terkmane Oussama

Zidane Djamel Eddine

Supervisor:

- **Dr.Abdelkarim Ammar**

Registration Number:……/2021

Acknowledgement:

In the name of Allah, the Most Gracious and the Most Merciful, Alhamdulillah, all praises to Allah for His Guidance and for giving us knowledge, health and will to accomplish this thesis.

We would like to express our deepest gratitude to our supervisor Dr. AMMAR Abdelkarim for his support, precious tips and valuable time throughout the project, despite all his responsibilities.

We would conclude with our deepest gratitude to our parents, and all our loved ones.

The work would have not been possible without their blessings and moral support.

Our special gratitude goes to our friend *BOUKORSI Nadhir* for being there for us whenever we needed him.

Abstract

Generally, the conversion from AC to DC uses conventional uncontrollable or controllable diodes rectifier in both single phase and three phases. The main drawbacks of these rectifiers are injecting a huge amount of distortion in the AC-side line currents, low power factor and high ripple factor in the output DC- side. Recently, new types of controllable AC to DC converters such as PWM rectifier and Vienna rectifier which improve the quality of AC- line current with a low harmonics distortion, high power factor that is almost unity and a straight output DC- current which reduce ripple factor.

This thesis is interested in comparison study between PWM rectifier and Vienna rectifier. Both structures and principle of work of these rectifiers are presented and what are factors that control them. It also covers the SVM (space vector modulation) and how this technique is different from a rectifier to another. Finally, the performance of PWM and Vienna rectifiers are evaluated under several control strategies such voltage oriented control (VOC) and model predictive control- finite control set (MPC-FCS) that reduce the complexity of previous control strategy. The performances are tested under different conditions balanced, unbalanced and distorted network. All covered techniques are simulated using MATLAB/Simulink software.

Key words: PWM rectifier, Vienna rectifier, harmonics distortion, space vector modulation, voltage oriented control, predictive control.

Table of contents

Chapter III

Voltage Oriented Control of PWM and VIENNA rectifiers

Chapter IV

Model predictive control of PWM and VIENNA rectifiers

List of figures

List of tables

List of abbreviations

AC	Alternative Current
CCS	Continuous Control Set
DC	Direct Current
DSVM	Discrete Space Vector Modulation
DPC	Direct Power Control
DTC	Direct Torque Control
FCS	Finite Control Set
FOC	Field Oriented Control
HSVM	Hybrid Space Vector Modulation
IEC	International Electrotechnical Commission
IEEE	Institute of Electrical and Electronic Engineers
MOSFET	Metal Oxide Semi-conductor Field Effect Transistor
MPC	Model Predictive Control
PLL	Phase Locked Loop
PV	Photo Voltaic
PE	Power Electronics
PI	Proportional-Integral
PWM	Pulse Width Modulation
RMS	Root Mean Square
SVM	Space Vector Modulation
SVPWM	Space Vector Pulse Width Modulation

SPWM	Sinusoidal Pulse Width Modulation
THD	Total Harmonic Distortion
UPF	Unity Power Factor
VFOC	Virtual Field Oriented Control
VF	Virtual Flux
VOC	Voltage Oriented Control
ZSPWM	Zero Sequence Pulse Width Modulation

General Introduction

Background

In modern industry, power conversion is needed in many occasions. Most of AC-to-DC converters use Diode or Thyristor rectifiers. This kind of rectifiers injects many current harmonics into the network. Furthermore, they always consume reactive power (i.e. have low power factor) and require large amount of input and output filters for good performance [1].

To solve these issues new types of rectifiers have been widely used in recent years. The most famous ones are PWM rectifier and Vienna rectifier. Basically, PWM rectifier has many advantages include bi-directional power flow, nearly sinusoidal input current, regulation of input power factor to unity, low harmonic distortion of line current, adjustment and stabilization of DC-link voltage (or current) [2]. However, Vienna rectifier offer many other advantages include requiring fewer active switching components in producing the same number of voltage levels, and low device voltage stress, low control complexity and low sensing effort in terms of control system design and implementation. Therefore, the Vienna rectifier potentially reduces cost and provides more design flexibility for industry applications [3].

To ensure the achievement of the desired performance many control methods have been proposed that are: Voltage-Oriented-Control (VOC) [4], [5] and current Model Predictive Control-Finite Control Set (MPC-FCS) [6], [7], [8]. These two strategies are investigated to evaluate the performance of PWM rectifier and Vienna rectifier.

VOC is featured by controlling the active and reactive powers indirectly via two PI current control loops in dq-frame and one PI controller for DC-link. A Space Vector Modulator (SVM) generates switching signals at constant frequency. However, the structure of this strategy is rather complex [1]. The space vector modulation is totally different between PWM rectifier and Vienna rectifier. The main reason is that the degree of freedom in the Vienna rectifier is different than conventional converters. The conventional SVM which is used in PWM rectifier considers the

voltage vector as the primary vector which is used to locate the nearest switching states for the purpose of synthesizing the reference vector. Using the conventional SVM for the Vienna rectifier leads to a wrong selection of the nearest switching states [9].

To reduce the complexity of controlling, current MPC-FCS has been proposed which use only one PI controller for DC-link and no Space Vector Modulator (SVM) is required. In this control method, the discrete nature of power converters will be considered to optimize the number of calculations needed to achieve the optimum state [10]. The discrete nature of power can be modeled mathematically based on Euler's approximation at instant *k* for a sampling period T_s. the discretized mathematical model of PWM rectifier and Vienna rectifier are somehow similar the only difference is that discretized mathematical model of PWM rectifier depend only on the switching state. While, it depends on both switching state and lines current polarity for Vienna rectifier.

Objective and organization:

The main objective of this thesis is to make a comparison study between the performance of PWM rectifier and Vienna rectifier. For this reason, many control strategies may be used which can be categorized into traditional strategies such as voltage oriented control, direct power control and hysteresis control. The second category is the modern strategies that become widely used in recent years such as model predictive control and fuzzy logic control. All these strategies are used to mitigate harmonics distortion in the current AC-side, increase power factor and obtaining almost perfect DC current.

The first chapter covers power quality issues where the concept of THD is explained and how decreases power quality. It also discusses different classes of AC to DC rectifiers and their characteristics. Finally, a brief explanation of variant modulation techniques that used in rectifiers.

The second chapter describes the topology and principal of operation of both PWM and Vienna rectifiers. It explains also SVM and how it is different between the two rectifiers.

In the third chapter, first we give a general overview of different characteristics for conventional control strategies: VOC, VF-VOC, DPC, and VF-DPC. Secondly, we focus in concept of operation of VOC and we evaluate this strategy in improvement of performance for both PWM and Vienna rectifiers under balanced, unbalanced and distorted network.

In the last chapter, first we explain characteristics of model predictive control in both continuous control set and finite control set. Secondly, we focus in concept of operation of current MPC-FCS and we evaluate this strategy in improvement of performance for both PWM and Vienna rectifiers under balanced, unbalanced and distorted network.

Chapter I

State of art on power quality issues and AC-to-DC converters

1.1 Introduction

The aim of this chapter is to introduce electric power quality issues that come about disappointment or mis-operation of client equipment. These issues categories are discussed briefly. In this part we investigate harmonic problems that are mainly caused by AC to DC rectifiers, harmonics are most common and most bothersome of the power quality issues. The second part covers the operation of AC to DC three phase rectifiers. the last part covers the topology and variant modulation techniques that may be used for PWM rectifier.

1.2 Electric power quality

There are distinctive definitions for power quality. In IEEE (Institute of Electrical and Electronic Engineers) word reference, power quality is characterized as "the concept of powering and grounding sensitive equipment in a matter that is applicable to the operation of that equipment". In IEC dictionary (International Electrotechnical Commission), it is characterized as "set of parameters defining the properties of the power supply as delivered to the client in ordinary operating conditions in terms of continuity of supply and characteristics of voltage (magnitude, frequency, waveform).

The power supply system can only control the quality of the voltage; it has no control over the currents that particular loads might draw. Therefore, the standards in the power quality are related to maintaining the supply voltage within certain limits [11].

1.2.1 Power quality issues

Power quality issues are characterized as any power issue showed in voltage, current, or frequency deviations that come about disappointment or mis-operation of client equipment. Power quality problems can be categorized primarily into: Overvoltage, Undervoltage, Sags, Swells, Transients, Harmonics and Noise.

- **Overvoltage**: is known as the rise of the voltage in a circuit or part of above its upper design limit generally it is1.1 p.u. The conditions may be hazardous
- **Undervoltage**: is known as the decrease of the voltage in a circuit or part of under its lower design limit generally it is 0.9 p.u. **Fig.1.1** shows overvoltage and undervoltage events.

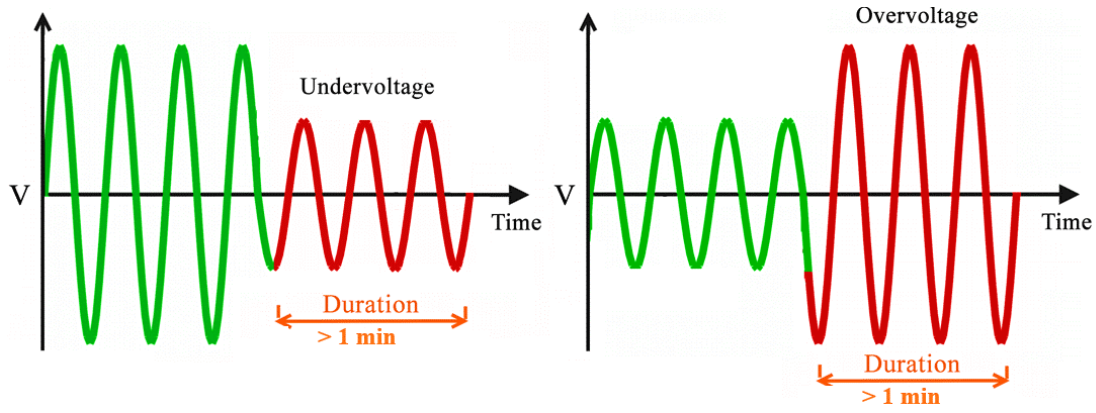

Fig1.1: Waveform shape during Undervoltage and Overvoltage events

- **Sag:** A decrease to between 0.1 and 0.9 pu in RMS voltage or current at the power frequency for durations of 0.5 cycle to 1 min. **Fig1.2** shows sag and swell event.
- **Swell**: a transitory increment within the RMS value of voltage of more than 10 percent of the nominal voltage at the frequency, for length from 0.5 cycle to 1 min.

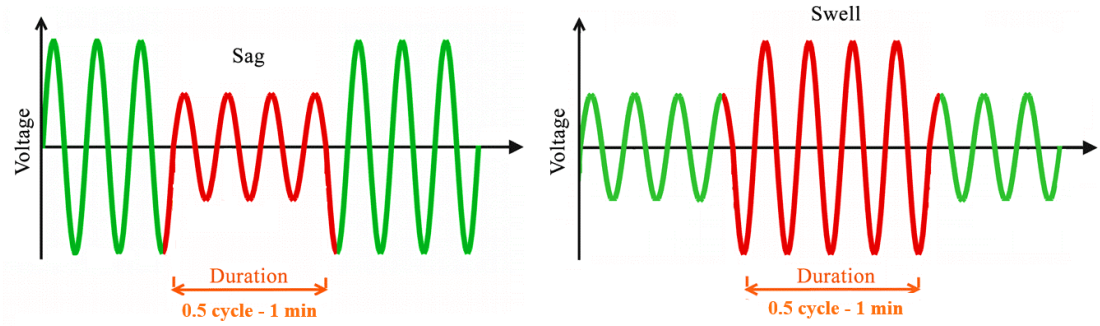

Fig.1.2: Waveform shape during Swell and Sag events

- **Transient:** Pertaining to or assigning a phenomenon or an amount that varies between two consecutive steady states during a time interval that is brief compared to the time scale of interest. A transient can be a unidirectional impulse of either polarity or a damped oscillatory wave with the first peak occurring in either polarity.
- **Harmonics:** Harmonics are sinusoidal voltages or currents having frequencies that are integer multiples of the supply frequency (fundamental frequency).
- **Noise:** Unwanted electrical signals that produce undesirable impact within the circuits of the control systems in which they happen.

1.2.2 Harmonics

Harmonics disturbances are the foremost critical of all power quality disturbances. They are defined as the substance of the signal whose frequency is an integer multiple of the system's fundamental frequency. Electricity is generated and supplied at 50 Hz in Algeria; Harmonics are multiples of the 50 Hz waves.

As harmonics are superimposed on the fundamental waveform, they distort the voltage and current waveforms, increase the current level and change the power factor of the supply, which in turn creates many disturbances since most electrical equipment are designed to handle smooth frequencies [12].

In order to estimate the harmonics displayed in a signal, Fourier series examination usually use the given signal that is either current or voltage. The signal f(ωt) is decomposed into: a DC component, fundamental frequency component and the harmonic frequencies components. F(ωt) in Fourier series shape is expressed as:

$$f(wt) = a_0 + \sum_{n=1}^{\infty}(a_n \cos(nwt) + b_n \sin(nwt)) \quad (1.1)$$

Where

$$a_0 = \frac{1}{2\pi}\int_0^{2\pi} f(wt)dwt \quad (1.1a)$$

$$a_n = \frac{1}{\pi}\int_0^{2\pi} f(wt)\cos(nwt)dwt \quad (1.1b)$$

$$b_n = \frac{1}{2\pi}\int_0^{2\pi} f(wt)\sin(nwt)dwt \quad (1.1c)$$

The total harmonic distortion THD is the amount of distortion in the waveform of f that is quantified by means of the index Total Harmonic Distortion (THD). It is given by the ratio of the rms of the total harmonic content to the rms value of the fundamental content:

$$THD = \sqrt{\frac{I_s}{I_{s1}} - 1}$$

The presence of harmonics has harmful effects on the power system's equipment as well as on its functioning reliability. The impacts of harmonics are summarized as follow [13]:

- **Decreased power factor:** harmonics increase the apparent power (S) required by the system, while the effective real power at the fundamental frequency does not benefit from that. This signifies that higher current is drawn, so added wire section and higher rating protection and distribution circuits are required.

- **Conductor losses:** obviously, additional current drawn apart from the needed at the fundamental frequency yields to additional cable losses at the conductors.

- **Skin effect:** the higher the frequency of the current passing through the wire, the higher its resistance losses.

- **Triplen harmonics and neutral conductor:** zero sequence harmonics (3^{rd}, 6^{th}, 9^{th},…etc.) also known as triplen harmonics circulate between phases and neutral. The presence of significant components of these harmonics can cause overheating. Unless the neutral is sufficiently oversized, a fire hazard may occur.

- **Resonance:** inductances and capacitors in the power system form resonant circuits. If this resonance is close to one of the harmonic frequencies injected, large current and voltage will be induced. This issue is especially related to capacitors bank installations for power factor correction.

- **Motors and generators:** the high impedance of generators will easily transfer current harmonic distortion into voltage harmonic distortion affecting other loads supplied from that source. The excessive shaft voltages and relevant bearing currents in motors fed from distorted supplies can cause bearing damage. Also, negative sequence harmonics tend to exert a force against torque rotation causing vibration, added heat and derating of motors. Extra core and copper losses are common effects of harmonics for both generators and motors.

- **Transformers:** the same effect of core losses and copper losses appear in transformers. Triplen harmonics in the neutral conductor of transformers can dangerously overheat them. There is also a potential risk of resonance between transformer inductance and supplied capacitive loads at some harmonic frequencies. Additionally, laminated transformers cores can vibrate at certain harmonic frequencies, causing audible noise and overheat.

- **Circuit breakers and fuses:** since tripping mechanism in circuit breakers and fuses

responds to rms current, a highly distorted current signal can cause false tripping and fusing and thus the need to oversize them which affects the sensitivity of the protection system.

1.3 AC to DC Rectifier

One of the first and most widely used application of power electronic devices have been rectification. Rectification refers to the process of converting an ac voltage or current source to dc voltage and current. Rectifiers specially refer to power electronic converters where the electrical power flows from the ac side to the dc side.

Rectifiers are used in a large variety of configurations and a method of classifying them into certain categories (based on common characteristics) will certainly help one to gain significant insight into their operation. Unfortunately, no consensus exists among experts regarding the criteria to be used for such classification. The classification shown in **Fig.1.3** will be followed.

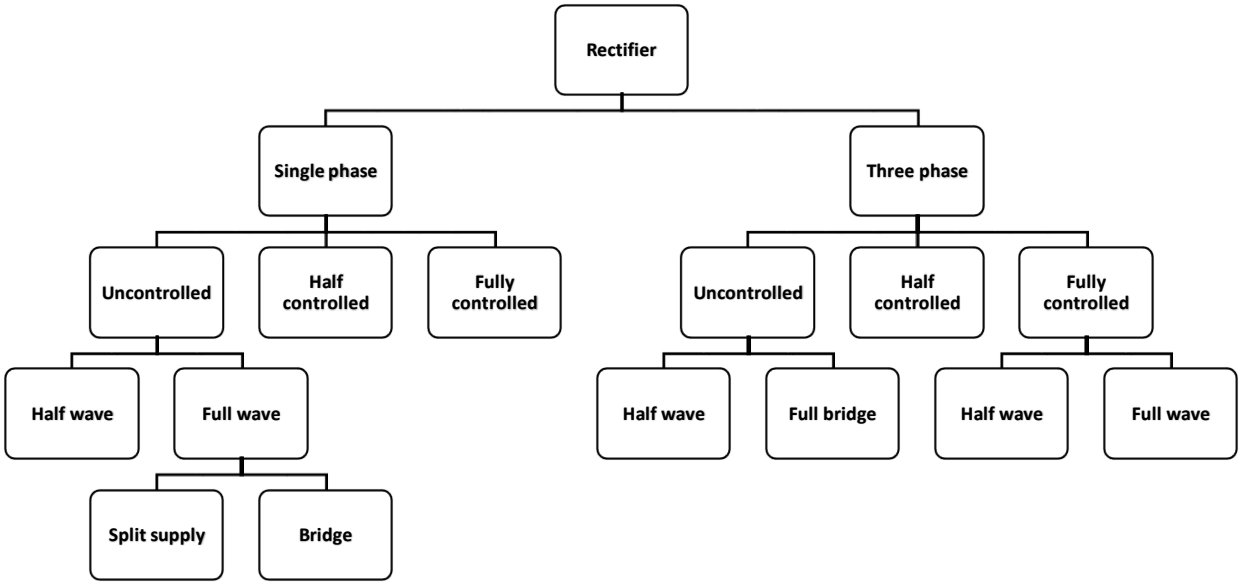

Fig.1.3 Classification of rectifiers

1.3.1 Three phase rectifiers uncontrolled rectifiers

1.3.1.a Three phase half wave uncontrolled rectifier

The circuit diagram of three phase half wave uncontrolled rectifier is shown in **Fig.1.4** It is clear that the diode whose line voltage is positively larger than other line voltage will be forward

biased while others remain reverse biased. Each diode conduct for a period of $\frac{2\pi}{3}$. **Fig.1.5** depicts output waveform for three phase half wave uncontrolled rectifier.

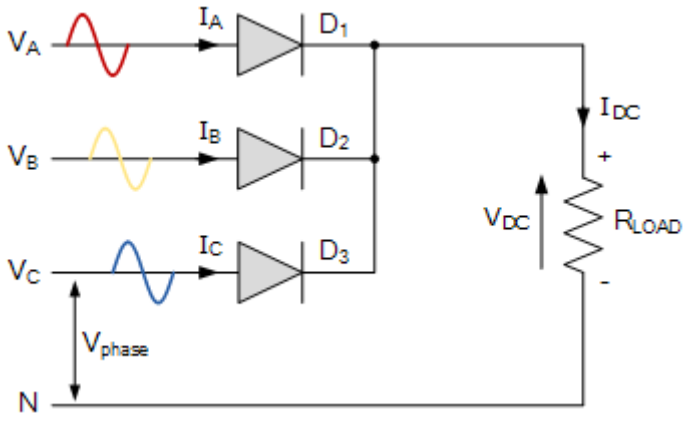

Fig.1.4: Three phase half wave uncontrolled rectifier

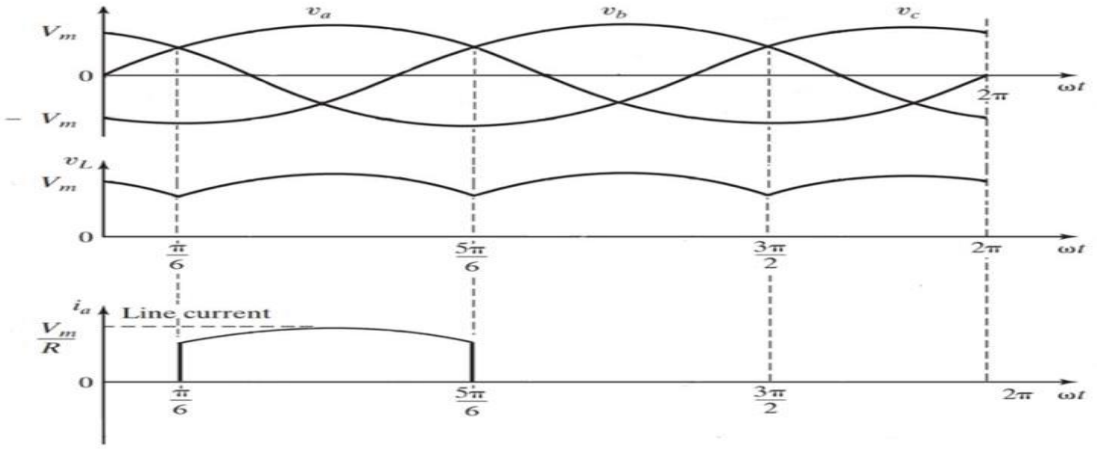

Fig.1.5: Output waveform of three phase half wave uncontrolled rectifier for resistive load

When wt $\in \left[\frac{\pi}{6}, \frac{5\pi}{6}\right]$ the output voltage equal to v_a since it is the greatest positive voltage:

The dc component and the rms value of the output voltage are given by:

$$V_{dc} = \frac{3}{2\pi}\int_{\pi/6}^{5\pi/6} V_m \sin(wt)\, dwt$$

$$V_{dc} = \frac{3\sqrt{3}V_m}{2\pi} \quad (1.2)$$

$$V_{rms} = \left[\frac{3}{2\pi}\int_{\pi/6}^{5\pi/6}(V_m \sin(wt))^2\, dwt\right]^{1/2}$$

$$V_{rms} = V_m\sqrt{\frac{\pi+0.75\sqrt{3}}{2\pi}} \qquad (1.3)$$

1.3.1.a Three phase full wave uncontrolled rectifier

The circuit diagram of three phase full wave uncontrolled rectifier is shown in **Fig.1.6** unlike to the three phase half wave uncontrolled rectifier the upper diodes D_1,D_5 and D_3 are conducting during positive half waves while lower diodes are conducting during negative half waves. Each diode conduct for a period of $\frac{\pi}{3}$. **Fig.1.7** depicts output waveform for three phase half wave uncontrolled rectifier

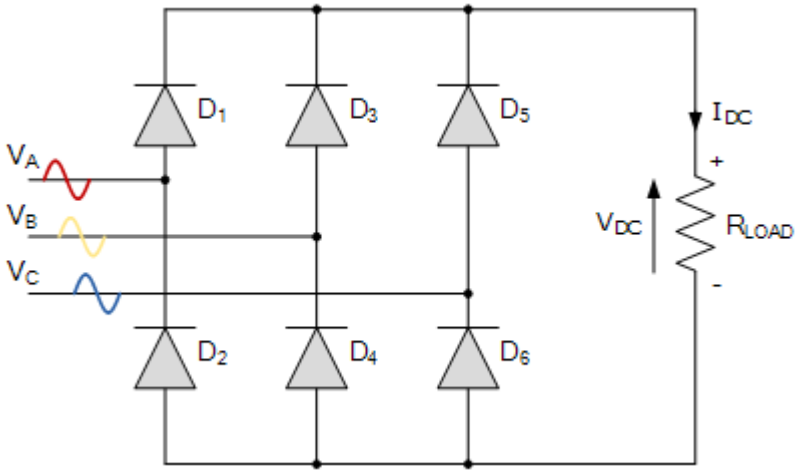

Fig.1.6: Three phase full wave uncontrolled rectifier

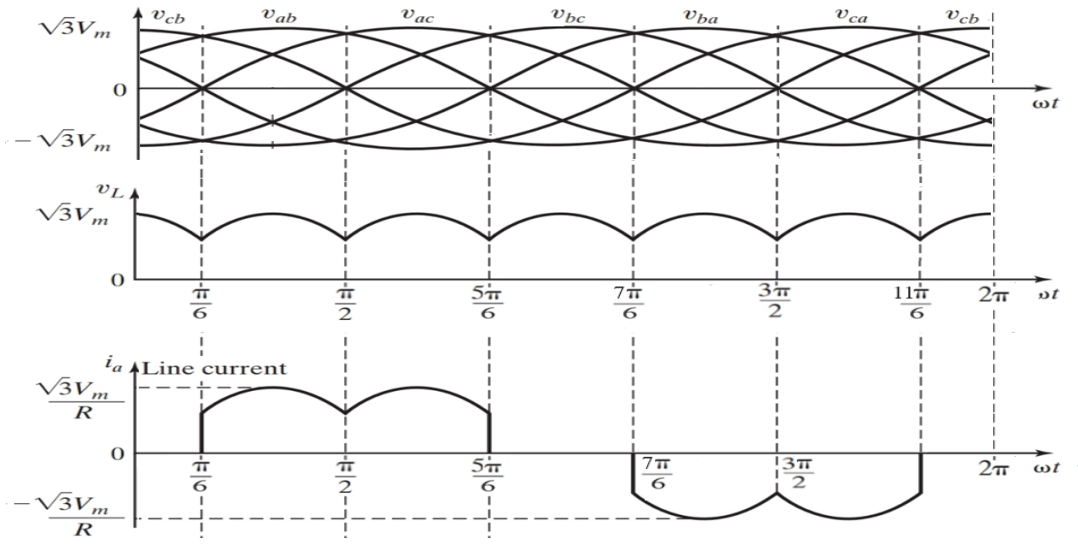

Fig.1.7 Output waveform of three phase full wave uncontrolled rectifier for resistive load

When wt $\in \left[\frac{\pi}{6}, \frac{\pi}{2}\right]$ the output voltage is given by:

$$V_L = v_{ab} = V_m \sin(wt + \frac{\pi}{6}) \tag{1.4}$$

The dc component and the rms value of the output voltage are given by:

$$V_{dc} = \frac{3}{\pi}\int_{\pi/6}^{\pi/2} \sqrt{3}V_m \sin(wt + \frac{\pi}{6})\, dwt$$

$$V_{dc} = \frac{3\sqrt{3}V_m}{\pi} \tag{1.5}$$

$$V_{rms} = \left[\frac{3}{\pi}\int_{\pi/6}^{\pi/2} (\sqrt{3}V_m \sin(wt))^2\, dwt\right]^{1/2}$$

$$V_{rms} = \sqrt{3}V_m\sqrt{\frac{0.5\pi+0.75\sqrt{3}}{\pi}} \tag{1.6}$$

1.3.2 Three phase full wave controlled rectifier

The circuit diagram of three phase full wave controlled rectifier is shown in **Fig.1.8** the upper SCRs will be on during positive half wave so they should be fired with an angle α in this period to conduct while the lower SCRs will be on during negative half wave so they should be

fired with an angle α in this period to conduct. The output voltage waveforms for inductive load are shown in **Fig.1.9**.

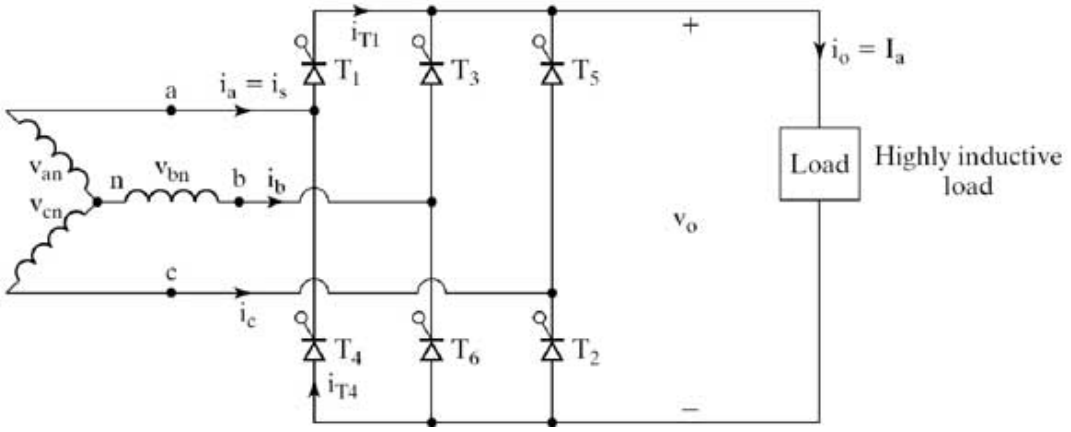

Fig.1.8 three phase full wave controlled rectifier

The table below summarize the operated SCRs during 2π and its interval time

SCR fired	Interval time	on	Output voltage
T 1	$\left[\frac{\pi}{6}+\alpha \rightarrow \frac{\pi}{6}+\frac{\pi}{3}+\alpha\right]$	T 1, T 6	$V_o = V_{ab}$
T 2	$\left[\frac{\pi}{6}+\frac{\pi}{3}+\alpha \rightarrow \frac{\pi}{6}+\frac{2\pi}{3}+\alpha\right]$	T 1, T 2	$V_o = V_{ac}$
T 3	$\left[\frac{\pi}{6}+\frac{2\pi}{3}+\alpha \rightarrow \frac{\pi}{6}+\pi+\alpha\right]$	T 3, T 2	$V_o = V_{bc}$
T 4	$\left[\frac{\pi}{6}+\pi+\alpha \rightarrow \frac{\pi}{6}+\frac{4\pi}{3}+\alpha\right]$	T 3, T 4	$V_o = V_{ba}$
T 5	$\left[\frac{\pi}{6}+\frac{4\pi}{3}+\alpha \rightarrow \frac{\pi}{6}+\frac{5\pi}{3}+\alpha\right]$	T 5, T 4	$V_o = V_{ca}$
T 6	$\left[\frac{\pi}{6}+\frac{5\pi}{3}+\alpha \rightarrow \frac{\pi}{6}+2\pi+\alpha\right]$	T 5, T 6	$V_o = V_{cb}$

Table 1.1 Operation of three phase full wave controlled rectifier

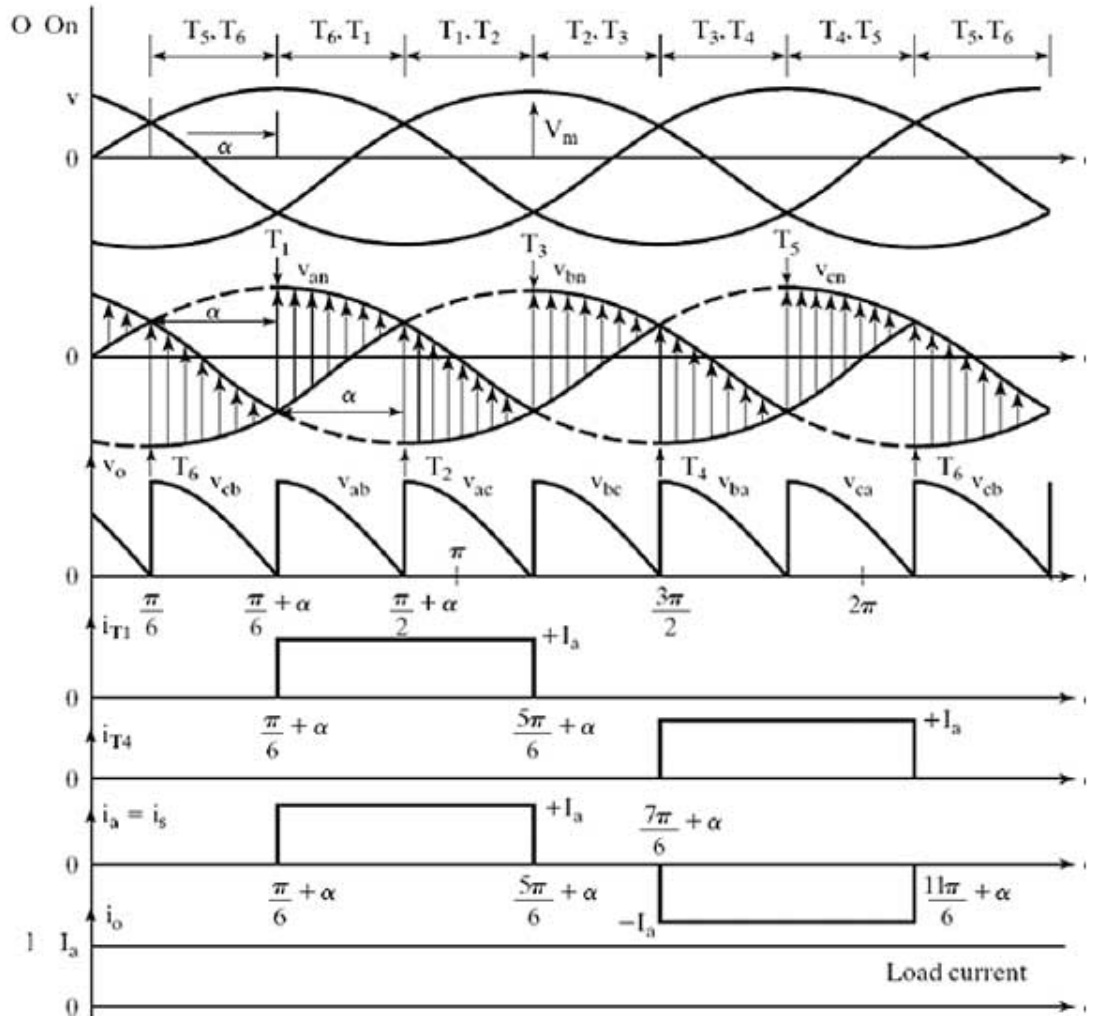

Fig.1.9 output waveform of three phase full wave controlled rectifier for inductive load

The dc component and the rms value of the output voltage are given by:

$$V_{dc} = \frac{3V_{mLL}}{\pi}\cos\alpha \tag{1.7}$$

$$V_{rms} = \sqrt{3}V_m\left(\frac{1}{2} + \frac{3\sqrt{3}}{4\pi}\cos 2\alpha\right)^{1/2} \tag{1.8}$$

1.3.3 Perturbation caused by rectifiers

The foremost serious perturbation caused by rectifiers influences the line current's power quality; the signal is no more continuous, periodic but distant from sinusoidal, meaning it contains a huge number of harmonics. The harmonic currents are reactive in nature which implies that they diminish the power factor of the system.

The output is not perfect DC that increases the ripple factor. this issue may be solved by connecting a capacitor in parallel with the output load. Rectifiers cause also voltage notching when commutated from one phase to another, a momentary short circuit between the lines is caused but it is not hazardeous. For single phase low voltage applications, the voltage drop of the diodes due to forward biasing perturbate the voltage waveform and decreases the efficiency of the system.

1.4 Topology of PWM rectifier

1.4.1 Description of switching state

The conventional 3-phase, PWM full controlled rectifier is illustrated in **Fig.1.10** consists of three legs with two active switches in each one. So, in total there are six active switches. The two switches of each leg "phase" can't be ON simultaneously. If this case is somehow occurring in the phase where it happen will be shorted when both switches are ON. However, both switches can be OFF simultaneously. In this case, it acts like uncontrolled rectifier. Based on that, if the upper switch of a certain phase is ON the lower switch should be necessarily OFF and vice versa.

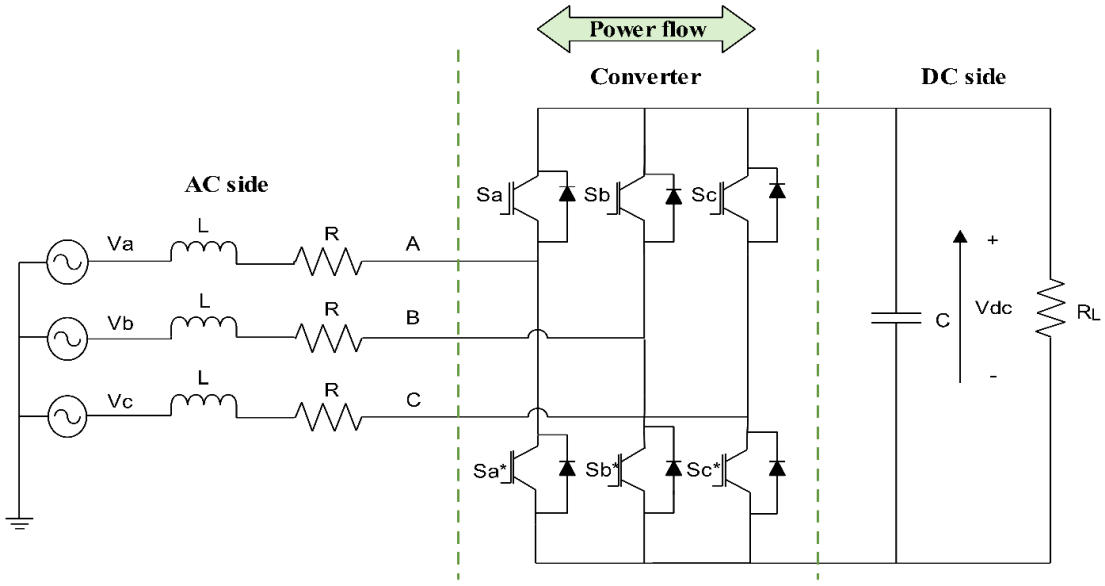

Fig.1.10 3-phase, PWM full controlled rectifier

The switching state for 3-phase, PWM full controlled rectifier. where 1 represent the ON state for the upper switch (A^+, B^+, C^+) and the OFF state of the lower switch (A^-, B^-, C^-) as well. While, 0 represent the OFF state of the upper switch and the ON state of the lower switch as well. Hence there are eight possible position of all switches that are illustrated in **Table.1.2**:

Switching state	A^+	A^-	B^+	B^-	C^+	C^-
000	OFF	ON	OFF	ON	OFF	ON
001	OFF	ON	OFF	ON	ON	OFF
010	OFF	ON	ON	OFF	OFF	ON
011	OFF	ON	ON	OFF	ON	OFF
100	ON	OFF	OFF	ON	OFF	ON
101	ON	OFF	OFF	ON	ON	OFF
110	ON	OFF	ON	OFF	OFF	ON
111	ON	OFF	ON	OFF	ON	OFF

Table 1.2 Switching state for 3-phase, PWM full controlled rectifier

1.4.2 Mathematical description for 3phase PWM rectifier

a. AC side description

The following figure represents the single-phase schematic of a three-phase PWM converter in rectification mode, where VL is the line voltage and U is the bridge converter.

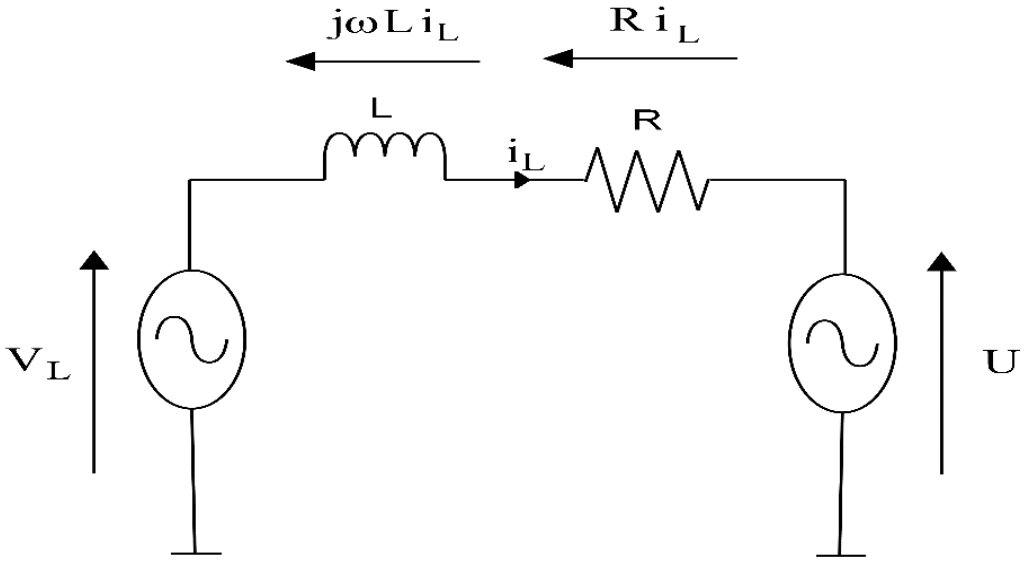

Fig.1.11 Single phase representation of the AC side of three phase PWM restifier

Applying the KVL to derive the voltage and current equations of the rectifier in three-phase reference frame:

$$\begin{bmatrix} V_a \\ V_b \\ V_c \end{bmatrix} = R \begin{bmatrix} i_a \\ i_b \\ i_c \end{bmatrix} + L \frac{d}{dt} \begin{bmatrix} i_a \\ i_b \\ i_c \end{bmatrix} + \begin{bmatrix} U_a \\ U_b \\ U_c \end{bmatrix} \quad (1.9)$$

b. DC side description

The figure below depicts the relation between converter voltage, switching states and the output voltage. The upper and lower IGBTs cannot be turned on simultaneously for it will cause a line short circuit, IGBTs conduct current in a single direction.

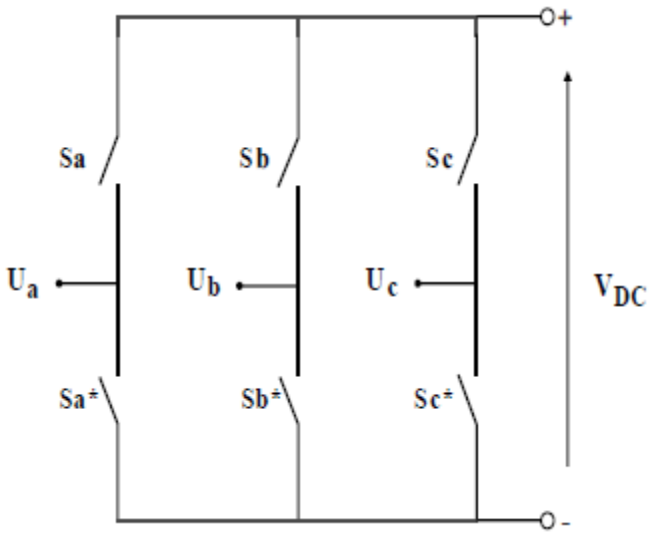

Fig.1.12 Relationship between converter voltage, switching states and the output voltage

When the upper switch 'S' is ON, the line current flows into the DC side through DU and the closed loop is completed by DL of one of the remaining arms, when lower switch 'S*' is ON, the current doesn't flow into the DC side, instead it loops back to the grid. **fig.1.13** shows the representation of arm current flow:

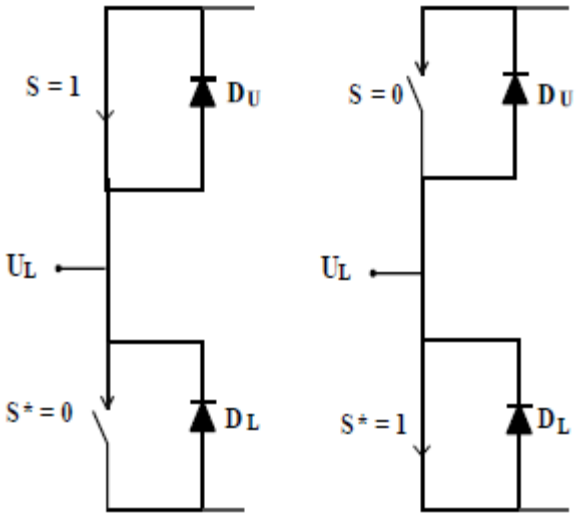

Fig.1.13 The representation of arm current flow

The relations between the currents as well as the converter voltage and the DC output are deduced as follow:

$$C\frac{dV_C}{dt} = S_a i_a + S_b i_b + S_c i_c - -i_{load} \tag{1.10}$$

$$U_{ab} = (S_a - S_b).V_{dc} \tag{1.11a}$$

$$U_{bc} = (S_b - S_c).V_{dc} \tag{1.11b}$$

$$U_{ac} = (S_a - S_c).V_{dc} \tag{1.11c}$$

From equations (1.11a), (1.11b) and (1.11c):

$$\begin{bmatrix} U_a \\ U_b \\ U_c \end{bmatrix} = \frac{V_{dc}}{3}.\begin{bmatrix} 2 & -1 & -1 \\ -1 & 2 & -1 \\ -1 & -1 & 2 \end{bmatrix}.\begin{bmatrix} S_a \\ S_b \\ S_c \end{bmatrix} \tag{1.12}$$

1.5 PWM techniques

Now-a-days, PE (Power Electronic) devices are most important in converting and controlling of electric power, particularly in extracting the renewable power like PV(Photovoltaic) arrays and wind energy [14]. The principle of a multi-carrier PWM method is to compare the modulating signal with a multi-carrier waveform of different levels, these are typically triangular waveforms. The carrier signal frequency denotes the switching frequency (fs) [14].

The frequency of a PWM signal must be much higher than that of the modulating signal, the fundamental frequency, such that the energy delivered depends mostly on the modulating signal. The advantage of PWM based switching power converter over linear power amplifier is [15]:

- Easy to implement and control.
- No temperature variation- and aging-caused drifting or degradation in linearity.
- Compatible with today's digital micro-processors
- Lower power dissipation.

Different PWM modulation techniques can be summarized as follow [16]:

Space vector PWM: In SVM case, the synchronously rotating reference vector V_{ref} as illustrated in **Fig.1.14** are used for taking sample in every sub-cycle, T_s . As a result, active voltage vector 1 (V_1), the active voltage vector 2 (V_2) and the zero vectors are obtained with applied time T1, T2 and T0 this will be discussed later in the next chapter.

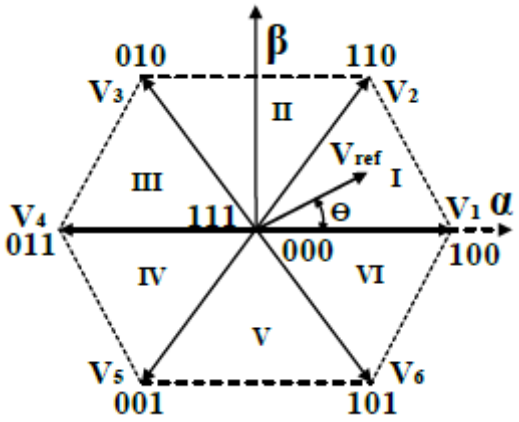

Fig.1.14 Voltage vectors produce by a two-level rectifier

Sinusoidal PWM: In this method, the reference wave is compared with high frequency triangular carrier wave and switching pulses are obtained and fed to the inverter's switches. The fundamental frequency is controlled by controlling modulating signal and its peak amplitude decides the modulation index. The modulation index is considered as a ratio of the peak magnitude of modulating wave to the fundamental peak of carrier wave. It provides lower fundamental output voltage as compared to SVPWM.

Zero sequence PWM: In this method, a Common mode third harmonic component is added in all the three sinusoidal waveforms. Advantage of the addition of these signal is that the sinusoidal modulating wave can have an amplitude above one without causing over modulation and it will result in 15% higher fundamental voltage. However, from the detailed analysis, it has been observed that when the amplitude of the common mode component is 1/6, then it will provide 15% higher fundamental voltage. But, when the amplitude of common mode component is 1/4, then it will provide only 11% higher voltage as compared to SPWM method.

Discrete SVM (DSVM): the main difference between CPWM and DSVM is that the only one null vector is applied for entire time duration T0. Different types of DSVM techniques are summarized below discussed below:

- **Negative 120 degree clamp (DSVM N120):** In DSVM N120, the clamping of 120° takes place at the canter of 180° to 360° for every 360° of fundamental voltage.
- **60 degree clamp (DSVM 60):** This type of switching sequence clamps each phase during the middle 60° duration and it is symmetrical in both positive and negative peaks of the modulating reference wave.
- **30 degree clamp (DSVM 30):** This type of switching sequence clamps each phase during the middle 30° symmetrically in every $1/4^{th}$ cycle of modulating reference wave.
- **15 degree clamp (DSVM 15):** This newly developed switching sequence clamps each phase during the every 15° symmetrically around the positive and negative peaks of its modulating reference wave.
- **Hybrid SVM (HSVM):** This newly developed switching sequence clamps each phase during the middle 45° duration and also symmetrical in both positive as well as negative peaks of its modulating reference wave.

1.6 Space vector modulation of PWM rectifier

The space vector modulation is another representation of the switching that have been discussed earlier. In this technique the reference voltages $\overrightarrow{V_{ref}}$ are given by space voltage vector and the output voltages of the inverter are considered as space vectors [17]. Applying the switching state to the converter, eight voltage vectors are obtained which correspond to the eight possible

states of the rectifier switches. Two of them are zero vectors $(\overrightarrow{V_0}, \overrightarrow{V_7})$ six voltage vectors are active vectors $(\overrightarrow{V_1}$ up to $\overrightarrow{V_6})$ that can be described mathematically as follow:

$$\overrightarrow{V_i} = \sqrt{\frac{2}{3}}\, V_{dc}\, e^{j(i-1)\frac{\pi}{3}} \quad i=1,2,\ldots 6 \tag{1.13}$$

The six active vectors divide a plane for the six sectors 1–6 as illustrated in **Fig.1.15**:

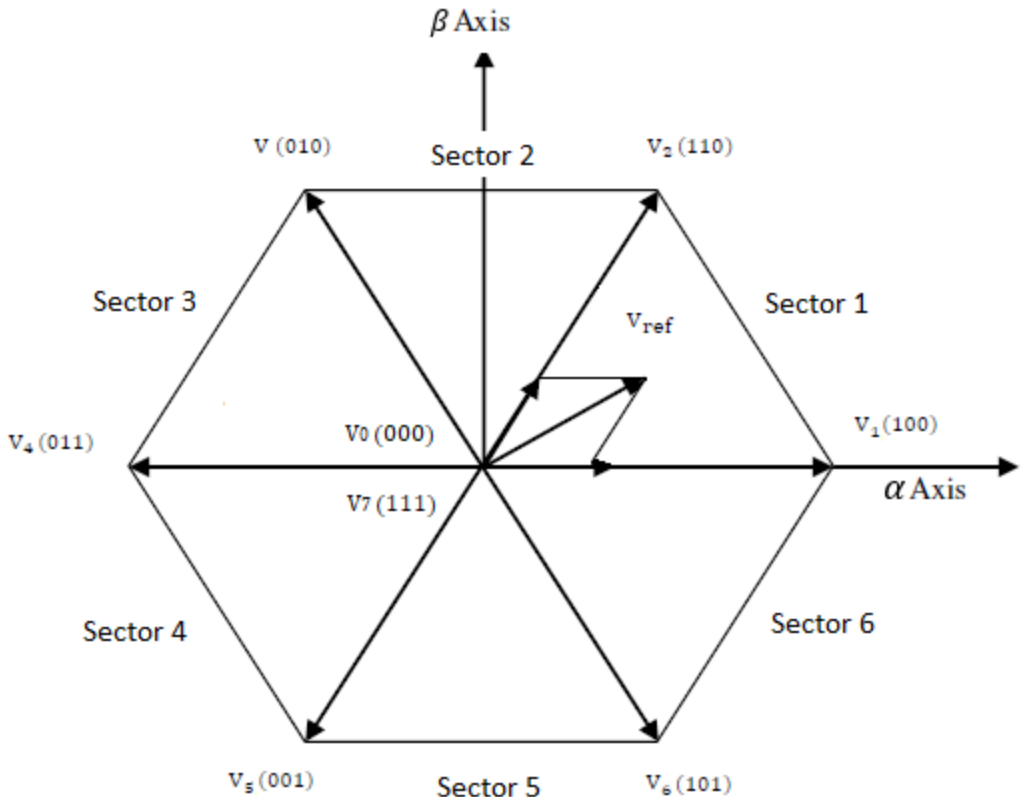

Fig.1.15 Space vector diagram for 2-level converter

The reference voltage vector is realized by the sequential switching of active and zero vectors. In each sector, the reference voltage vector $\overrightarrow{V_{ref}}$ is obtained by switching on two adjacent vectors [17]. these adjacent vectors are used to determine the dwell time or the ON time for the switching state. For instance if $\overrightarrow{V_{ref}}$ is located in sector 1 thus it is resultant of switching on $\overrightarrow{V_1}$ and $\overrightarrow{V_2}$. as shown in **Fig.1.16:**

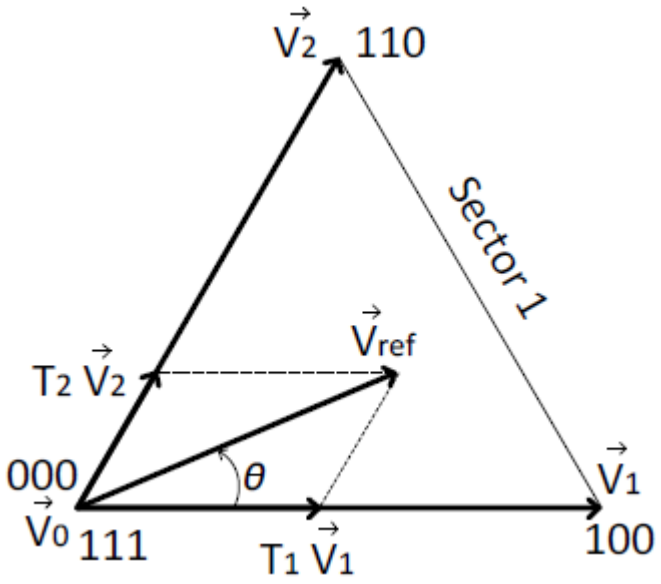

Fig.1.16 Approximating the reference space vector voltage using two active vectors and two zero vectors [18]

Using the definition of volt-second balance, equation (1.14) and (1.15) can be derived [18] :

$$T_s \overrightarrow{V_{ref}} = T_1\vec{V}_1 + T_2\vec{V}_2 + T_0\overrightarrow{V_0} \quad (1.14)$$

$$T_S = T_1 + T_2 + T_0 \quad (1.15)$$

T_0 ,T_1,T_2 are found using basic trigonometric relations as depicts in equations (1.16a), (1.16b), (1.16c) :

$$T_1 = \frac{\sqrt{3}}{V_{dc}} T_s |V_{ref}| \sin(60 - \theta) \quad (1.16a)$$

$$T_2 = \frac{\sqrt{3}}{V_{dc}} T_s |V_{ref}| \sin(\theta) \quad (1.16b)$$

$$T_0 = T_s - (T_1 + T_2) \quad (1.16c)$$

In **Fig.1.16**, the reference vector does not touch the boundary of the hexogen. As a result, the sum $T_1$of and T_2 is less than the switching time Ts , which means $\overrightarrow{V_0}$ must be applied for the remaining time of the switching period T_0. From equation (1.16a) to (1.16c), it can be deduced that the dwell time T_1 and T_2 are depend on the reference vector's angle. This relation is summarized in the following **Table.1.3**[18]:

Reference angle	0	$0 < \theta < 30$	$\theta = 30$	$30 < \theta < 60$	$\theta = 60$
Dwell time	$0 < T_1$ $T_2 = 0$	$0 < T_1 < T_2$	$T_1 = T_2$	$0 < T_2 < T_1$	$0 < T_2$ $T_1 = 0$

Table 1.3 Relation between the reference vector's angle and dwell time in sector 1

The calculation of the switching times (duty cycles) is expressed as follows [19]:

Upper side:

$$Taon = T1 + T2 + T0/2 \quad (1.17a)$$

$$Tbon = T2 + T0/2 \quad (1.17b)$$

$$Tcon = T0/2 \quad (1.17c)$$

Lower side:

$$Taon = T0/2 \quad (1.18a)$$

$$Tbon = T1 + T0/2 \quad (1.18b)$$

$$Tcon = T1 + T2 + T0/2 \quad (1.18c)$$

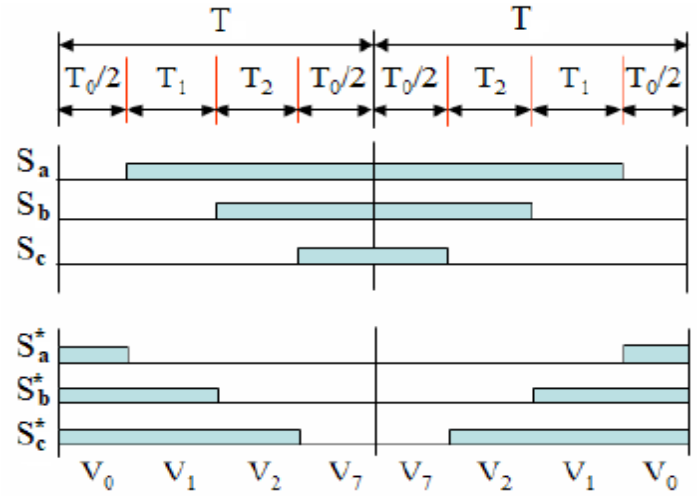

Fig.1.17 Switching times for sector 1 [19]

1.7 Conclusion:

In this chapter, we have covered major power quality issues especially harmonics since it is caused by AC/DC converter. Later it discusses different types of rectifiers where we focus on three phase controlled and uncontrolled rectifier. The last part devotes to principle of operation for PWM rectifier also it compares between variant type of PWM techniques. Finally, we explain space vector modulation technique for PWM rectifier.

Chapter II

Topology and SVPWM of VIENNA rectifier

2.1 Introduction

The aim of this chapter is to introduce 3 phase AC-DC Vienna rectifier. first we give a general description. The topology and modes of operation of Vienna rectifier in details. a simplified Space Vector Pulse Width Modulation (SVPWM) technique for the Vienna rectifier presented.

2.2 Introduction to Vienna rectifier

Vienna rectifier was first invented in 1993 by Johan W. Kolar. **Fig.2.1** illustrates the most famous circuit topology of the three-phase Vienna rectifier, which consists of a six diodes (D_1 to D_6), three controllable switches (S_a, S_b, S_c), three input filter inductors, and two dc-link capacitors (C_1, C_2). It is widely used in many applications such that in industrial applications such as telecommunication systems, aircraft, power factor correction systems [20] due to its advantages over conventional rectifier [21]:

- Has continuous sinusoidal input current.
- Low-blocking voltage stress on the power transistors.
- High power density.
- High efficiency.
- Low complexity of the power and control circuit.
- High reliability.
- Resistive main behavior.
- Controlled output voltage.

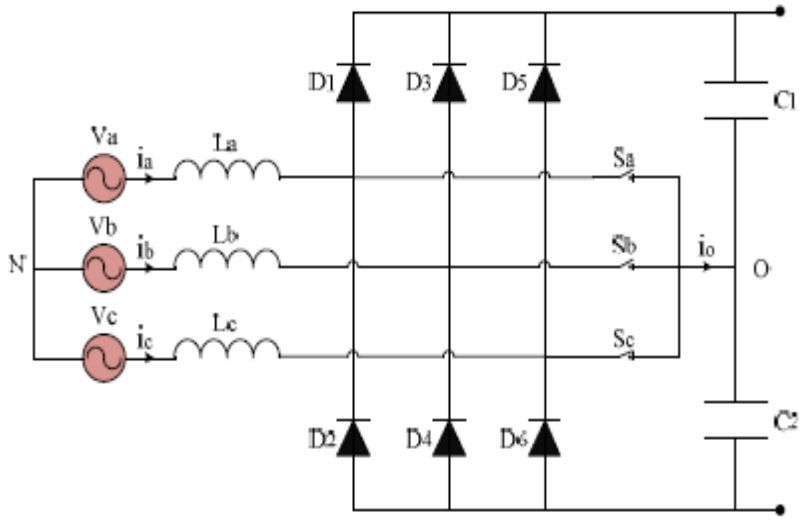

Fig.2.1 Schematic of Vienna rectifier [22]

In particular, the rectifier-side voltages (U_{ao}, U_{bo} and U_{co} referred to the midpoint O) are not only related to the controllable switching states but also the polarities of associated input currents, which is due to that the Vienna rectifier is current force commutated [22]. Based on that the following cases are distinguished:

- If a certain switch S_i (i=a,b,c) is ON this switch is clamped to the associated leg and $V_{io} = 0$.
- If a certain switch S_i (i=a,b,c) is OFF V_{io} depends on the polarity of the associated input current if the current is positive $V_{io} = V_{dc}/2$ else $V_{io} = -V_{dc}/2$.
- $V_{dc}/2$, $V_{dc}/2$, 0 are the three applicable voltages the rectifier-side that is why it is known as a 3-level converter.

2.3 Topology of Vienna rectifier

The equivalent switches (S_a, S_b, S_c) can be modeled as bidirectional bipolar switches as depicted in **Fig.2.2**. where P1 and P4 are connected to the input inductance and the midpoint O respectively. While P2 and P3 are connected to the upper and lower diodes respectively.

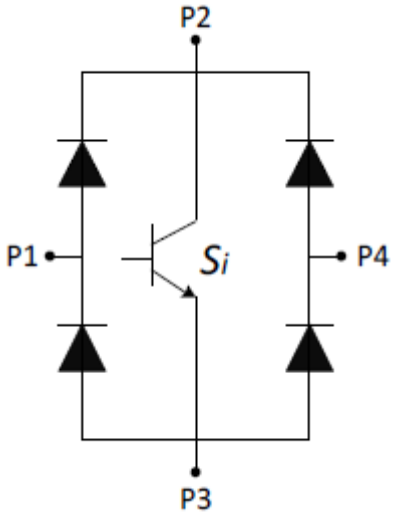

Fig.2.2 Bidirectional bipolar switch

The flow of current through the switch depends on the polarity of the current and the state of the switch (ON or OFF) based on that four different paths can be taken by the current:

- When the transistor S is turned ON and the current is positive the current flow from P1 to P4 through diodes DS_1 and DS_4 (1)
- When the transistor S is turned ON and the current is negative the current flow from P4 to P1 through diodes $DS_2$and DS_3 (2)
- When the transistor S is turned OFF and the current is positive the current flow from P1 to P2 through diode DS_1 (3)
- When the transistor S is turned OFF and the current is positive the current flow from P3 to P1 through diode DS_4 (4)

All these paths are summarized in the following set of **fig.2.3**:

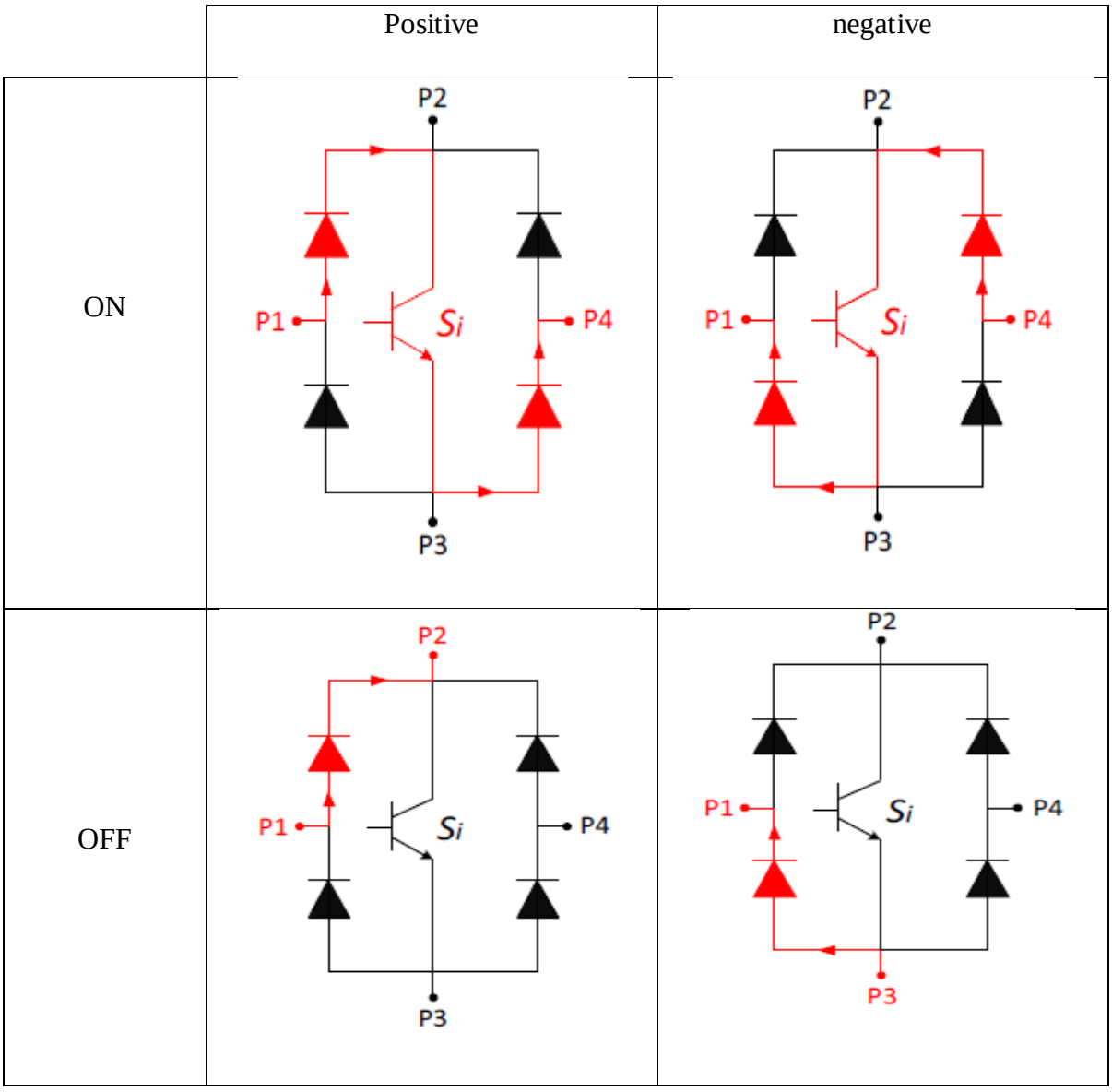

Fig.2.3 Different paths for current flow in the switch

2.4 operation of Vienna rectifier

Since Vienna rectifier has a three switches there are eight possible switching state ($2^3 = 8$). As a three phase system, considering the polarity of currents there are six possible sectors which are represented in **Table.2.1**. Combining the eight possible switching state with the six sectors we get 48 possible operation modes. some of these modes are repeated thus this will end up with only 25 operation mode. These will be discussed in the next section.

	A	B	C
Sector 1	+	-	-
Sector 2	+	+	-
Sector 3	-	+	-
Sector 4	-	+	+
Sector 5	-	-	+
Sector 6	+	-	+

Table 2.1 Polarity of currents in each sector

the input current of the rectifier has three paths to travel through, depending on the current direction and the active switches status [18]:

- The first path is from the rectifier's input to the midpoint through the upper diode in the case of positive current and OFF switch thus the upper capacitor C1 boosts the positive voltage.
- The second path is from the lower capacitor C2 to input's rectifier through the lower diode in the case of negative current and OFF switch.
- The third path is through the active switch where the direction is from the input inductor to the midpoint and vice versa governed by the polarity of the current.

Fig.2.4, **Fig.2.5**, **Fig.2.6** and **Fig.2.7** show the different paths for phase a [23]:

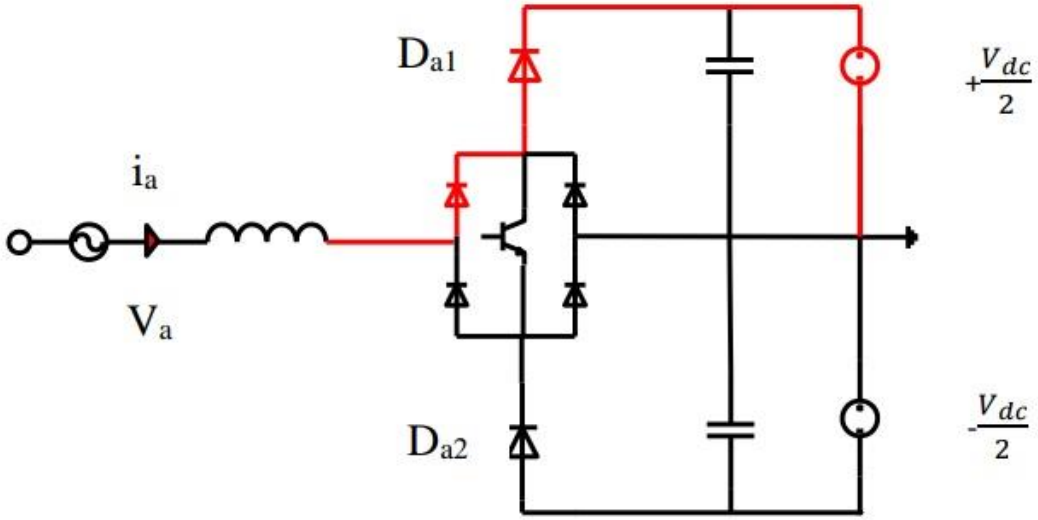

Fig.2.4 Line current is positive and S_a is OFF (first path)

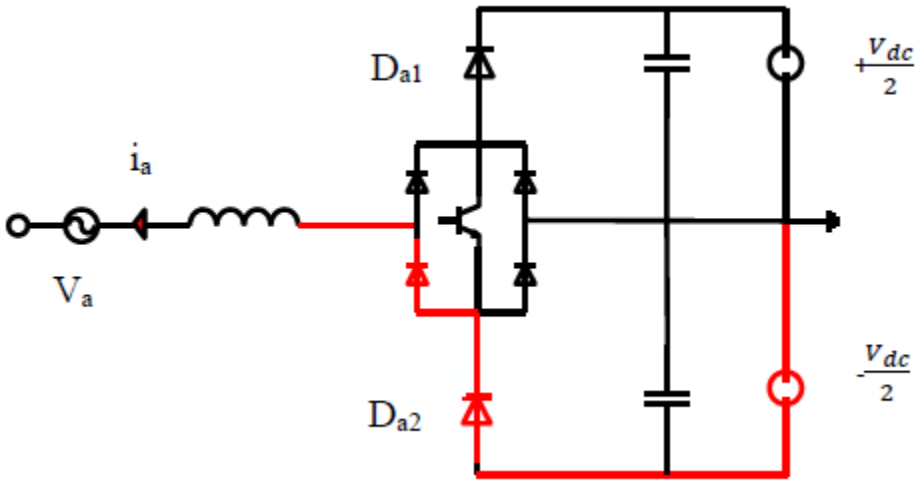

Fig.2.5 Line current is negative and S_a IS OFF (second path)

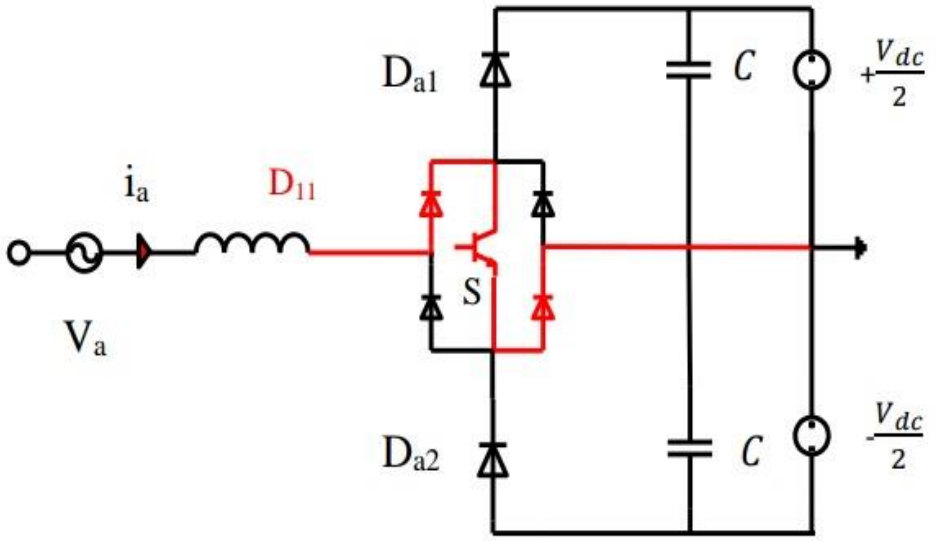

Fig.2.6 Line current is positive and S_a is ON (third path)

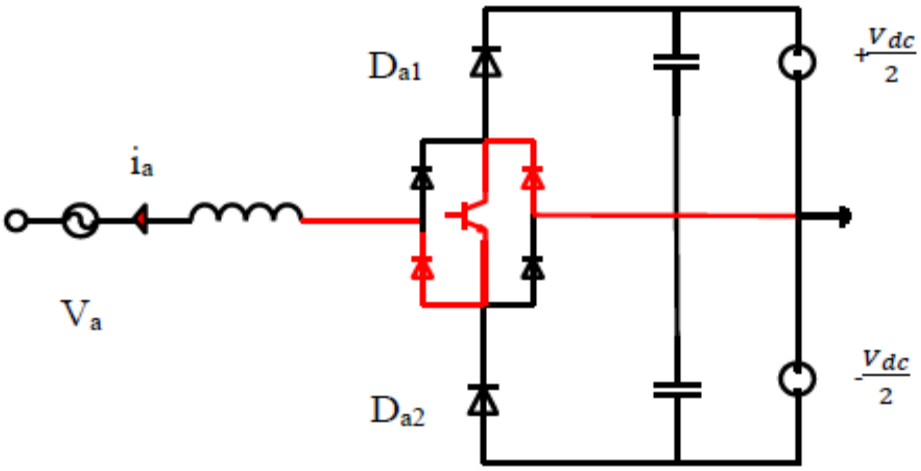

Fig.2.7 Line current is negative and S_a is ON (third path)

Current paths of switching position 001 and currents polarity $+--$ (sector1) is shown in **Fig.2.8**:

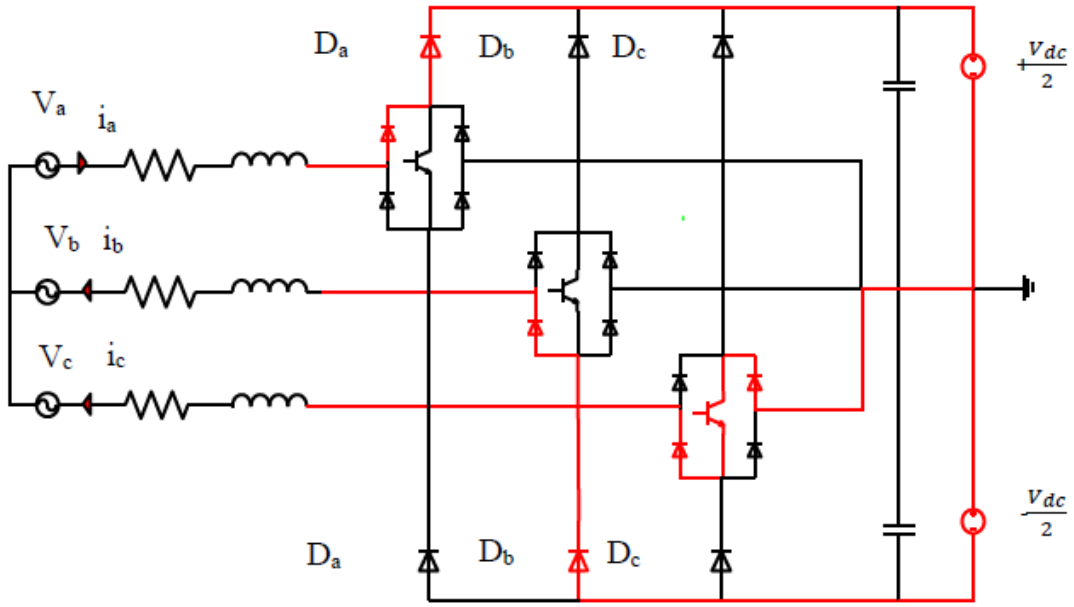

Fig.2.8 Current paths of switching position 001 and currents polarity $+--$ (sector1)

2.5 SVM for Vienna rectifier

Using the conventional SVPWM for the Vienna rectifier leads to a wrong selection of the nearest switching states since the polarity of the phase currents choose which voltage level is to be applied. In other words, when applying the conventional SV method, not all voltage space vectors are visible at a given time because the direction of the phase current limits the applicable voltage space vectors. Therefore, the SVPWM for the Vienna rectifier uses the current vector as the primary vector [18].

To facilitate modeling, denote S_i as each controllable switching state. $S_i = 0$ means the switch S_i is OFF, while $S_i = 1$ denotes ON. For the sake of convenience, V_{io} could be performed in a compact way as [22]:

$$\begin{cases} V_{ao} = K_a \frac{V_{dc}}{2} \\ V_{bo} = K_b \frac{V_{dc}}{2} \\ V_{ao} = K_a \frac{V_{dc}}{2} \end{cases} \quad (2.1)$$

Where K_i is switching function is represented as:

$$\begin{cases} K_a = \text{sign}(i_a)(1 - S_a) \\ K_b = \text{sign}(i_B)(1 - S_b) \\ K_C = \text{sign}(i_C)(1 - S_c) \end{cases} \quad (2.2)$$

Where $\text{sign}(i_i)$ is the the polarity of the associated current phase. It is +1 if the polarity is positive and it is -1 if the polarity is negative. Based on that:

- if S_i is ON K_i should be necessarily 0 whatever the polarity of i_i thus V_{ao}=0.
- if S_i is OFF K_i equal to $\text{sign}(i_i)$

as discussed earlier in section 2.3, there are only 25 operation modes for Vienna rectifier. Investigating equation (2.2) all possible different values that K_i can be taken are summarized in **Table.2.2**:

Section	000	100	001	101	010	110	011	111
1	+1,-1,-1	0,-1,-1	+1,-1,0	0,-1,0	+1,0,-1	0,0,-1	+1,0,0	000
2	+1,+1,-1	0,+1,-1	+1,+1,0	0,+1,0	+1,0,-1	0,0,-1	+1,0,0	000
3	-1,+1,-1	0,+1,-1	-1,+1,0	0,+1,0	-1,0,-1	0,0,-1	-1,0,0	000
4	-1,+1,+1	0,+1,+1	-1,+1,0	0,+1,0	-1,0,+1	0,0,+1	-1,0,0	000
5	-1,-1,+1	0,-1,+1	-1,-1,0	0,-1,0	-1,0,+1	0,0,+1	-1,0,0	000
6	+1,-1,+1	0,-1,+1	-1,-1,0	0,-1,0	-1,0,+1	0,0,+1	-1,0,0	000

Table 2.2 Results of switching function in each sector [18]

It is remarkable that there are repeated switching function for the same switching state in different sections. As example, for switching state “011” the switching function “+1,0,0” is repeated twice in section1 and 2. For the same switching state, the switching function “-1,0,0” is repeated four times from section 3 to 6. Counting all possible repeated switching function. we end up with 25 possible functions which represent the different operation modes.

2.5.1 Space vector for Vienna rectifier

The following equation describes the voltage at the input of the rectifier system with respect to the capacitor mid-point (o):

$$V_{io} = K_a \frac{V_{dc}}{2} \tag{2.3}$$

Moreover, the voltage between the neutral point (N) and the capacitor midpoint (o) can be calculated in equation (2.4) [9]:

$$V_{No} = \frac{V_{dc}}{6} (K_a + K_b + K_c) \tag{2.4}$$

Thus the voltage at the input of the rectifier system with respect to the Neutral point (N) as shown in equation (2.5) [9]:

$$V_{iN} = V_{io} - V_{No} \tag{2.5}$$

Therefore, the voltage space vectors of the Vienna rectifier are determined using one of these equations[9]:

$$\vec{V} = \frac{2}{3}(V_{aN}e^{J0} + V_{bN}e^{J\frac{2\pi}{3}} + V_{cN}e^{-J\frac{2\pi}{3}}) \tag{2.6a}$$

$$\vec{V} = \frac{2}{3}(V_{ao}e^{J0} + V_{bo}e^{J\frac{2\pi}{3}} + V_{co}e^{-J\frac{2\pi}{3}}) \tag{2.6b}$$

$$\vec{V} = \frac{V_{dc}}{3}(K_a e^{J0} + K_b e^{J\frac{2\pi}{3}} + K_C e^{-J\frac{2\pi}{3}}) \tag{2.6c}$$

All of equations presented above are illustrated graphically as shown in **Fig.2.9**:

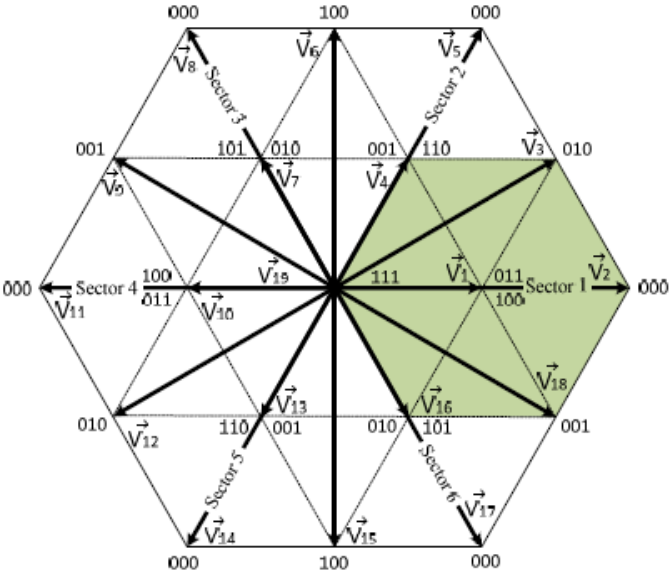

Fig.2.9 Space vector diagram for 3-level converters [9]

As could be noticed the Space vector diagram for Vienna rectifier is totally different from the Space vector diagram for PWM converters that have been covered in the previous chapter. Since the SVPWM for the Vienna rectifier uses the current vector as the primary vector.

As **fig.2.9** depicts, there are four different vector lengths and a total of 19 vectors:

- 6 of these vectors are called long vectors $\frac{2}{3}V_{dc}$.its switching states are always 000
- 6 are known as medium vectors $\sqrt{\frac{2}{3}}V_{dc}$.
- 6 are known as short vectors $\frac{1}{3}V_{dc}$, each of these vector has two redundant switching states.
- last vector is the zero vector which is located at the center of the hexagon. Its switching state is 111.

Fig.2.9 also shows that there are six sectors. Each sector is represented by a smaller hexagons located inside the big hexagon. This makes sector overlap with its adjacent sectors. As example sector 1 intersect with sectors 2 and 6. The center of each sector has a short vector.

Another representation of SVPWM for Vienna rectifier is illustrated in **fig.2.10**:

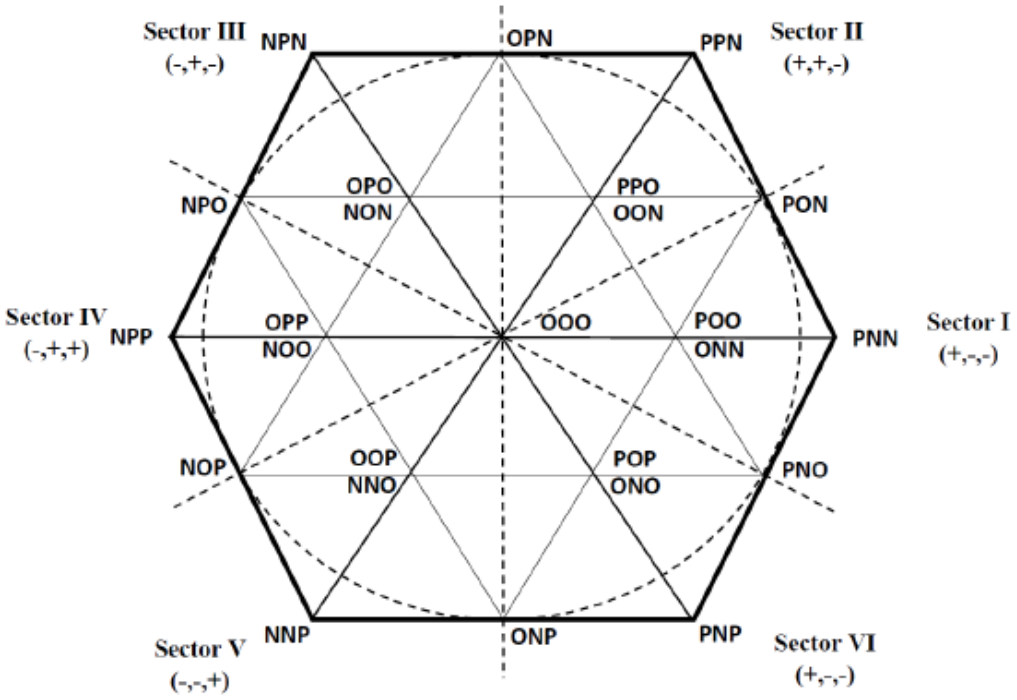

Fig.2.10 Vector diagram of Vienna rectifier

Where P indicates that the polarity of the current is positive and the switch is off, N indicates that the polarity of the current is negative and the switch is off and O indicate the ON state for switch.

2.6 pulse generation

Normalizing the angle (Φ) is defined in equation (2.7) and also shown in **Fig.2.11** which is a significant step to simplify the SVPWM for the Vienna rectifier. The main idea of angle normalization is to rotate the voltage vector, which is located in Sectors 2 to 6, to Sector 1; then, the calculations are performed on the basis of Sector 1 [9]:

$$\Phi = \theta - \frac{\pi(N-1)}{3} \tag{2.7}$$

Where N is the sector number and the target vector V_{ref_old} is located. Rotating this vector to sector 1. we get the new vector and its corresponding V_{ref} as illustrated in **fig.2.11**. thus forming an equivalent two level modulation region [24]:

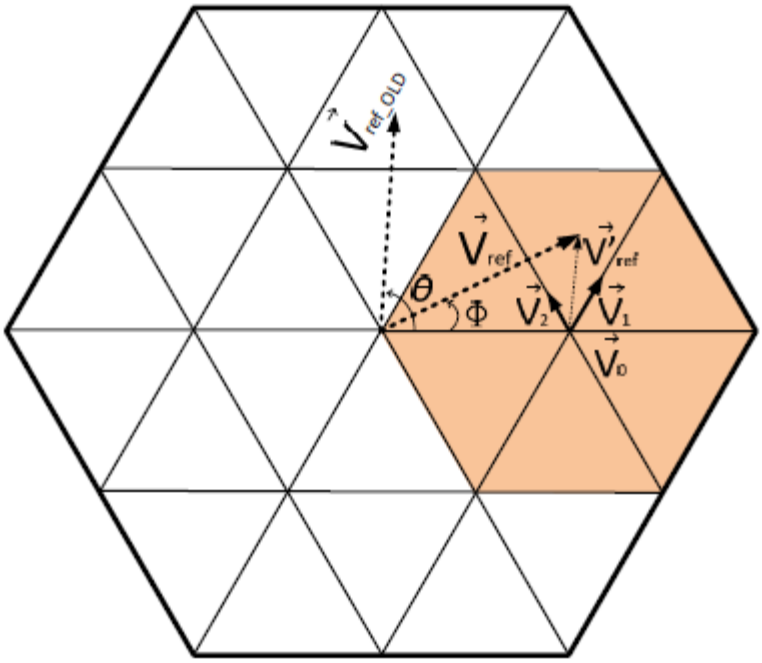

Fig.2.11 Example of angle normalization [9]

Vector action time fluxes X, Y, Z are introduced. T in equation (2.8) is the switching period, Vα, Vβ are the components of V′ref on the αβ axis, and Vdc is the DC-side output voltage vector [24]:

$$\begin{cases} X = \frac{2\sqrt{3}V_\beta}{V_{dc}} T \\ Y = \frac{3V_\alpha - \sqrt{3}V_\beta}{V_{dc}} T \\ Z = \frac{3V_\alpha + \sqrt{3}V_\beta}{V_{dc}} T \end{cases} \quad (2.8)$$

The vector interaction time of each small sector is shown in **Table.2.3**. T1 and T2 are the time of two nonzero vectors acting, and T0 is the time of the action of equivalent zero vectors

Sector	**1**	**2**	**3**	**4**	**5**	**6**
T1	Y	Z	X	-Y	-Z	-X
T2	X	-Y	-Z	-X	Y	Z
T0	T-T1-T2					

Table 2.3 Vector action time in each vector [24]:

A good DC output is mainly featured by a low current ripple factor to achieve that the vector action sequence should satisfy the following principles:

- When the action vector changes, there is only one phase switch action changes at a time as illustrated in **fig.2.11**. For instance, in triangle (1) when the switching state change from 000 to 010 switches a and c maintain. only switch b changes its station from 0 to 1. when the switching state change from 010 to 011 only switch c change it station from 0 to 1.
- The switch state at the beginning and at the end of a switch cycle is the same. According to the above principle, a seven segment vector synthesis method is adopted, and the switching state is symmetrical during the switching period. As shown in **fig.2.12**

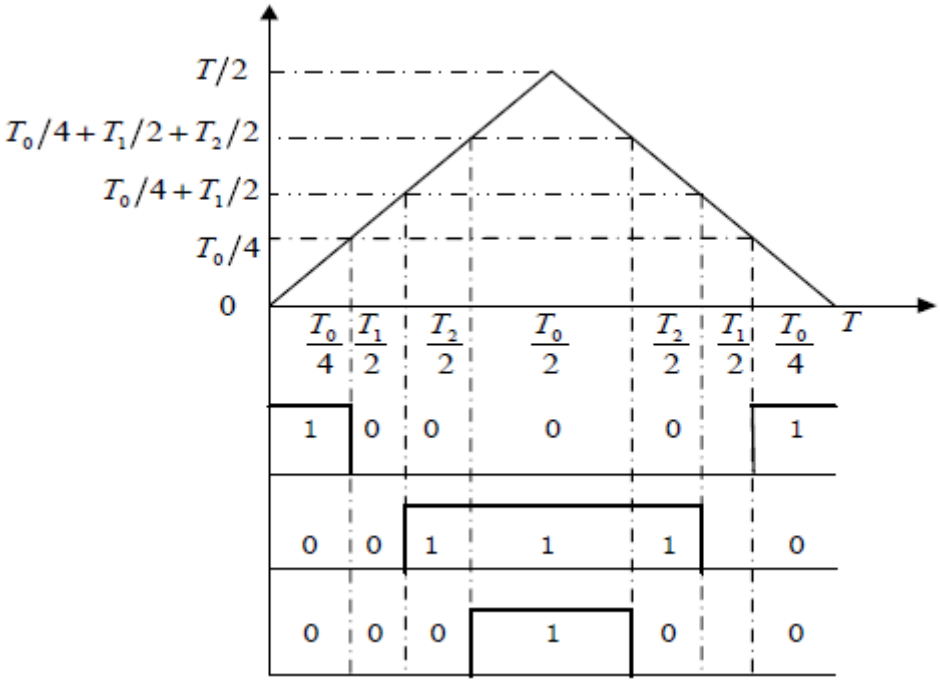

Fig.2.12 PWM in the first sector [24]

2.7 Conclusion:

Vienna rectifier has fewer switches compared to PWM rectifier that reduce the cost and make the control much easier. The operation of PWM rectifier depends only on the switching state while the operation of Vienna rectifier depends on both switching and the polarity of phases current. Applying SVPWM for the Vienna rectifier differs from the conventional converters since the active switches do not directly control the applied voltage level. Because of the degree of freedom in the Vienna rectifier is different than conventional converters. Thus, there are eight voltage vectors in SVPWM for PWM rectifier while there are nineteen feasible voltage vectors for Vienna rectifier.

Chapter III

Voltage Oriented Control of PWM and VIENNA rectifiers

3.1 Introduvtion

PWM rectifier has been widely used for many industrial applications. The switching pattern depends on external reference signal which is created according to the required voltage, current or power. Many control strategies are proposed for PWM rectifier.

This chapter first present features of the most common conventional control techniques: voltage oriented control (VOC), direct power control (DPC), virtual flux based control (VF). Then it describes the mathematical model of Vienna rectifier in d-q coordinates. After that voltage oriented control (VOC) is discussed deeply where its analogy is well covered. Finally, the control schemes are simulated in SIMULINK for PWM and Vienna rectifiers. The simulation results and major differences between the two rectifiers are discussed in order to deduce the merits and demerits of each rectifier.

3.2 PWM control schemes

The switching pattern of PWM rectifiers are generated based on external reference signal, this signal is created by the controller depending on the required voltage, current or power [25]. The figure bellow shows the control loop:

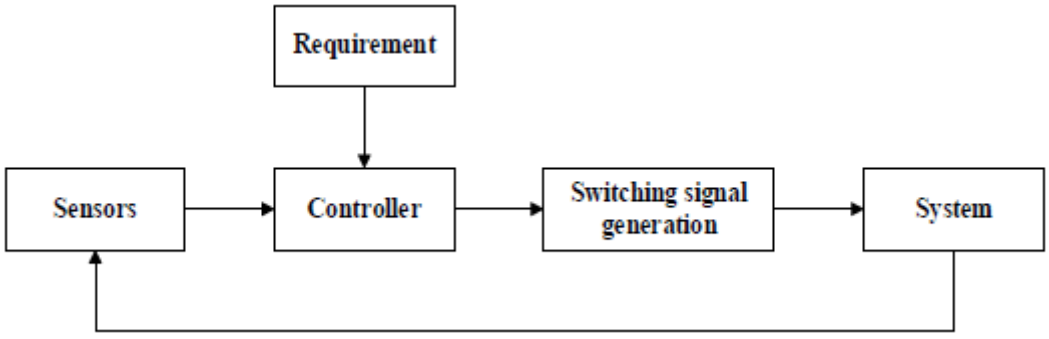

Fig.3.1 Control loop overview [1]

Extensive research has been conducted on rectifier control schemes in the past few years. Furthermore, several control approaches have been presented for the Vienna-type rectifier. These approaches include the hysteresis current control method, constant-frequency integration control scheme, conventional direct power control strategy, and unity power factor control method [3]. In our thesis we cover only voltage oriented control for the Vienna rectifier:

There is a such duality between PWM rectifiers control and induction motor control as illustrated in **fig.3.2**. In each control strategy there are different electrical quantities to be controlled (currents, voltages, powers). For voltage oriented control these quantities are currents as will be discussed in next sections:

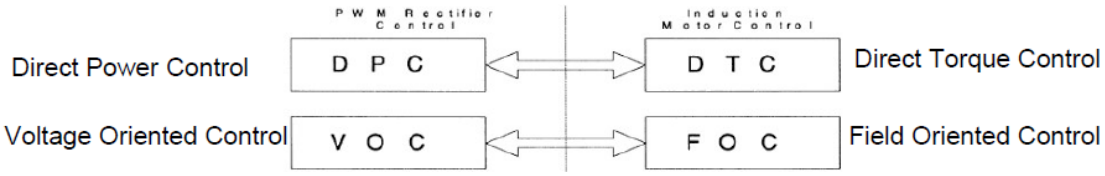

Fig.3.2 Duality between PMM rectifier and IM control technique [26]

3.3 Conventional control strategies for PWM rectifiers

In recent years many control strategies are developed for rectifiers.in order to achieve good power quality, low THD, low ripple factor, unity power factor in order to keep grid input voltage sinusoidal the most useful are illustrated in **fig.3.3**

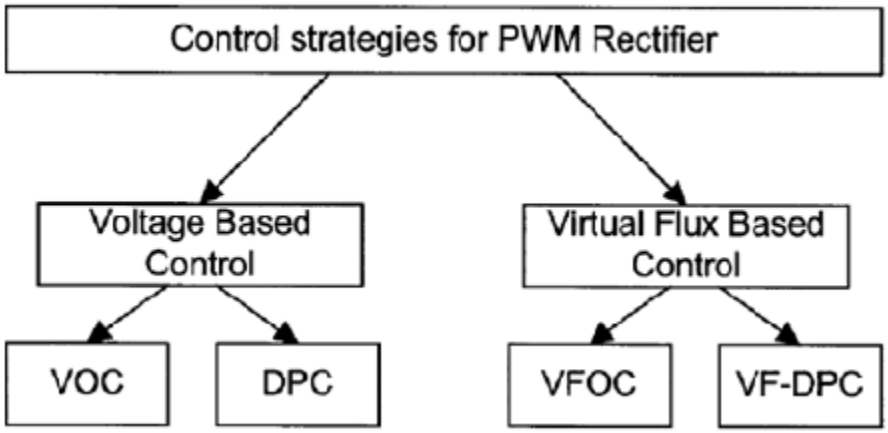

Fig.3.3 Control strategies [27]

- **The voltage oriented control (VOC):**

It guarantees high dynamic and static performance via an internal current control loop. But the quality depends mainly on the current control strategy [28].

- **The Direct Power Control (DPC):**

is based on the instantaneous active and reactive power control loop. There are no internal current control loop and no PWM modulator block. The switching state are determined with a

switching table based on the instantaneous errors between the commanded and estimated values of active and reactive power [28].

- **The Virtual Flux Based Control (VF-):**
  correspond to a direct analogy of IM control [28].

The following table summarize the main differences among the mentioned control strategies:

Feature	VOC	VFOC	DPC	VDPC
Direct control of	Line currents	Line currents	Line powers	Line powers
Estimation of	Power, line voltage	Virtual flux, Power	Power, line voltage	Power, line flux
Co-ordinate transform	Two	Two	_	_
PI controller	Yes (3)	Yes	No	No
Decoupling blocks	Yes	Yes	No	No
SVM modulator	Yes	Yes	No	No
Computational effort	high	high	Low	Low
Line voltage sensorless	Yes	Yes	Yes	Yes

Table 3.1 Rectifier control comparaison [26]

3.4 Mathematical model of Vienna rectifier in d-q coordinates

Fig.3.4 depicts the general topology of Vienna rectifier. As discussed earlier in section 2.2 the rectifier-side voltages (U_{aN}; U_{bN} and U_{cN}, referred to the voltage at the input of the rectifier system with respect to the capacitor mid-point (N)). Voltage across the switch is highly related to the state of switches and the polarity of input currents.

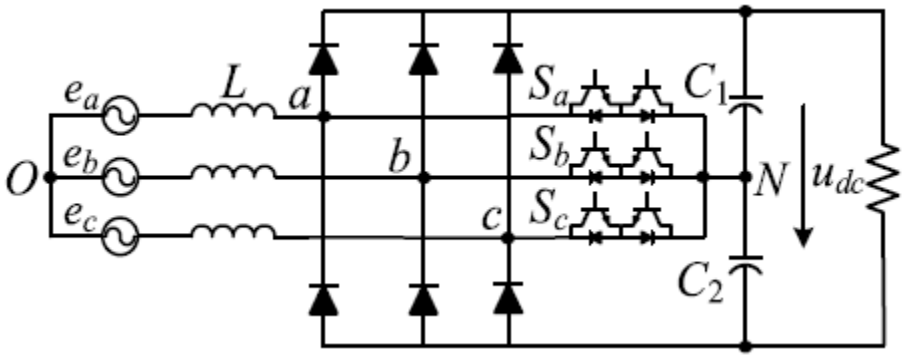

Fig.3.4 Circuit topology of the 3-phase Vienna rectifier

while, **Fig.3.5** illustrates its simplified equivalent circuit:

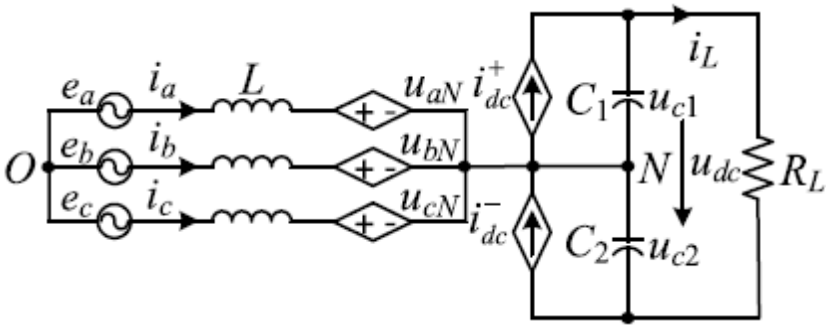

Fig.3.5 Equivalent circuit of the Vienna rectifier [22]

According to this scheme the mathematical of Vienna rectifier can be derived by applying KVL as following:

$$\begin{cases} L\frac{di_a}{dt} = e_a - Ri_a - U_{aN} \\ L\frac{di_b}{dt} = e_b - Ri_b - U_{bN} \\ L\frac{di_c}{dt} = e_c - Ri_c - U_{cN} \end{cases} \quad [22] \qquad (3.1)$$

Where L is input filter inductance; R is the line resistance; and e_i and i_i (i=a,b,c) are the grid-side voltages and input currents, respectively. as have seen earlier in section 2.6 the rectifier-side voltagesV_{iN} can be expressed as

$$V_{iN} = K_i \frac{V_{dc}}{2} \qquad (3.2)$$

Where K_i is the switching function of its associated phase it can represented as :

$$K_i = \text{sign}(i_i)(1 - S_i) \tag{3.3}$$

Where $\text{sign}(i_i)$ is the polarity of current i_i (positive or negative) and S_i is the switching state ('1' if it is ON and '0' if it is OFF)

Mathematically it is difficult to solve equation (3.1). Moreover, it is hard to design a controller in terms of this equation. To solve this issue equation (3.1) are transferred from 3 phase to dq coordinate using park's transformation as shown in equation (3.4):

$$\begin{cases} L\frac{di_d}{dt} = e_d - Ri_d + wLi_q - u_d \\ L\frac{di_q}{dt} = e_q - Ri_q - wLi_d - u_q \end{cases} \tag{3.4}$$

where the subscripts d and q imply the d-q axis components, respectively. w is the grid frequency.

Active and reactive powers can be expressed as follow [22]:

$$\begin{cases} P = 1.5(e_d i_d + e_q i_q) \\ Q = 1.5(e_q i_d - e_d i_q) \end{cases} \tag{3.5}$$

For a balanced three phase system $e_q = 0$ if i_q is controlled such way to be equal 0, Q=0 thus achieve unity power factor

3.5 Voltage oriented control

Prior designs of AC/DC converters for high power applications employed a hybrid controller using conventional three-phase controlled rectifiers, which requires input and output filters with high rating to mitigate the input current THD. This leads to reduced efficiency and power density of the system [4]

Similarly as in FOC of an induction motor, the Voltage Oriented Control (VOC) and for line side PWM rectifier is based on coordinate transformation between stationary α, β and synchronous rotating d-q reference system[2].

Voltage Oriented Control (VOC) is a control scheme based on d-q synchronous rotating reference frame. Grid voltage vector e is oriented to the d-axis, which lags q-axis by 90 degrees. The current i_α, i_β is divided into id and iq , as shown in **Fig.3.6**. In order to achieve unity power

factor (UPF), iq should be controlled to be zero [29]. From this concept voltage oriented control takes its name

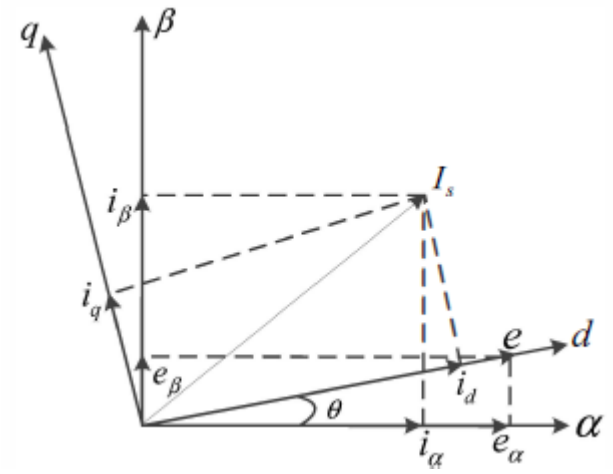

Fig.3.6 Vector diagram of the d-axis VOC

As illustrated in **fig.3.7** , grid voltages ($v_{s_{abc}}$) are measured in order to determine the oriented angle θ . a PLL can also be used to calculate this angle as illustrated in **fig.3.8**. The oriented angle θ is used in clark's and park's transformation as shown in equation (3.7):

$$\begin{bmatrix} V_{s\alpha} \\ V_{s\beta} \\ V_0 \end{bmatrix} = \sqrt{\frac{2}{3}} \begin{bmatrix} 1 & -\frac{1}{2} & -\frac{1}{2} \\ 0 & \sqrt{\frac{3}{2}} & -\sqrt{\frac{3}{2}} \\ \sqrt{\frac{1}{2}} & \sqrt{\frac{1}{2}} & \sqrt{\frac{1}{2}} \end{bmatrix} \begin{bmatrix} V_{sa} \\ V_{sb} \\ V_{sb} \end{bmatrix} \tag{3.6}$$

$$\begin{bmatrix} V_d \\ V_q \end{bmatrix} = \begin{bmatrix} \sin\theta & \cos\theta \\ -\cos\theta & \sin\theta \end{bmatrix} \begin{bmatrix} V_\alpha \\ V_\beta \end{bmatrix} \tag{3.7}$$

Line currents voltages ($i_{s_{abc}}$) are measured and then transformed to the d-q coordinates where the resultants i_{sd}, i_{sq} represent the actual measured currents.

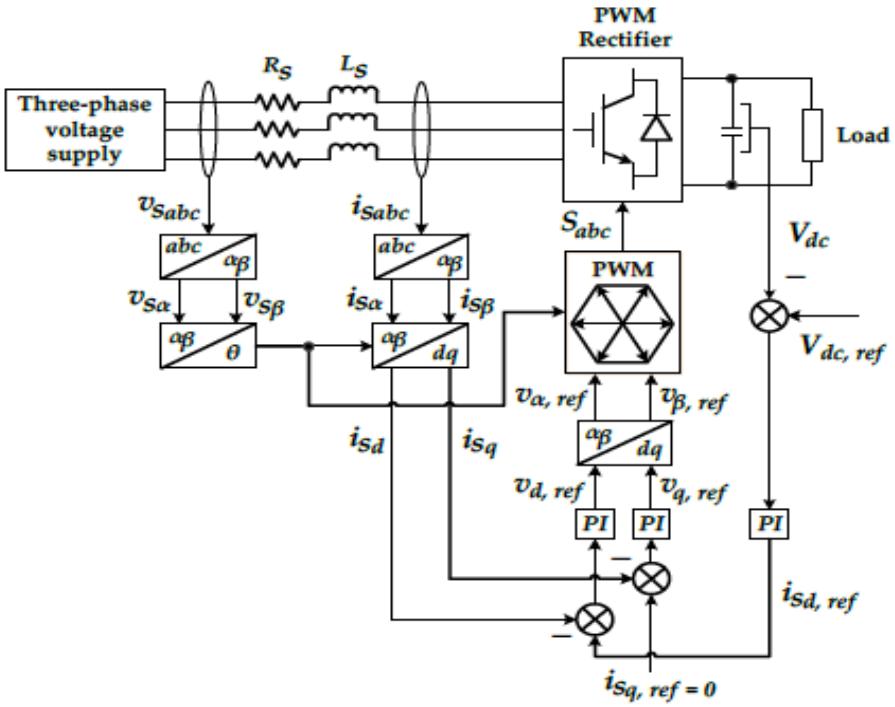

Fig.3.7 Overall control structure of voltage oriented control for PWM rectifier

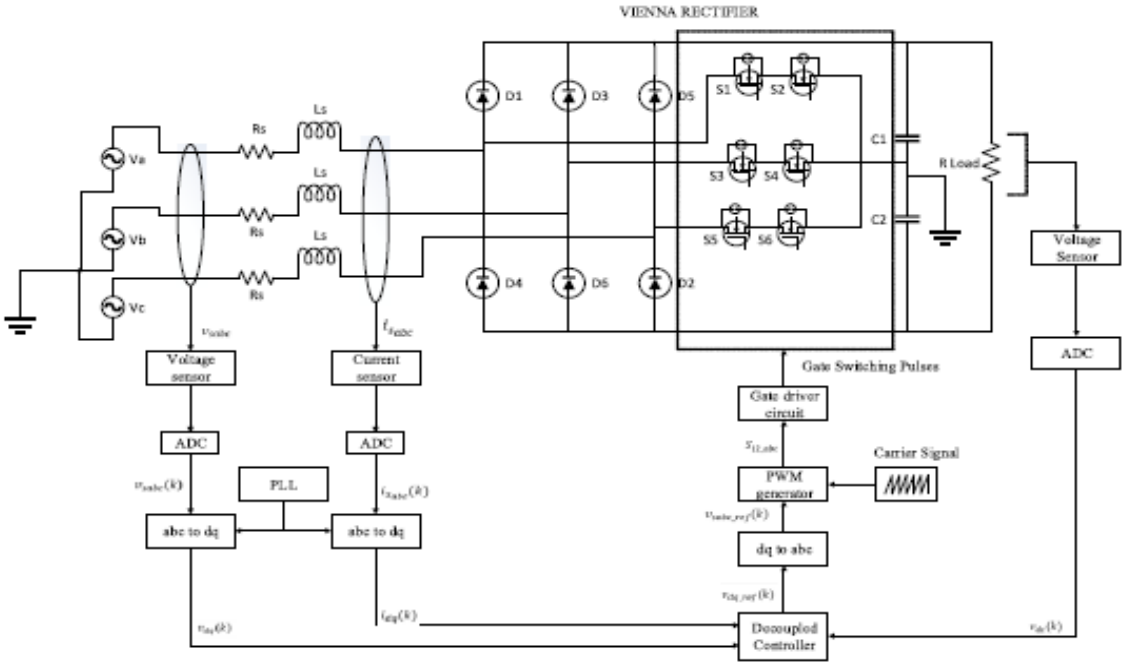

Fig.3.8 Overall Circuit Configuration of the proposed VOC-VR system.

The command active current $i_{d-ref(k)}$ which is the output of the dc-link can be described in the following equation:

$$i_{d-ref} = K_{p1}(V_{dc-ref} - V_{dc}) + K_{i1}\int(V_{dc-ref} - V_{dc})dt \quad (3.8)$$

Where K_{p1}, K_{i1} are the gain values of the PI voltage controller.

The command reactive current i_{q-ref} is set to be 0 to achieve UPF where it is compared to the actual reactive current i_q. the difference processed through a PI current controller to produce the voltage reference v_{q-ref} as described in equation(3.9):

$$v_{q-ref} = v_q + 2\pi f L_s i_q - (K_{p3}(i_{q-ref} - i_q) + K_{i3}\int(i_{q-ref} - i_q)dt) \quad (3.9)$$

Where K_{p3}, K_{i3} are the gain values of the PI current controller.

While, the active current i_{d-ref} is compared to the actual active current i_d. the difference processed through a PI current controller to produce the voltage reference v_{d-ref}as described in equation(3.10):

$$v_{d-ref} = v_d + 2\pi f L_s i_q - (K_{p2}(i_{d-ref} - i_d) + K_{i2}\int(i_{d-ref} - i_d)dt) \quad (3.10)$$

Where K_{p2}, K_{i2} are the gain values of PI current controller.

The figure below summarizes the overall control circuit of the decoupled controller

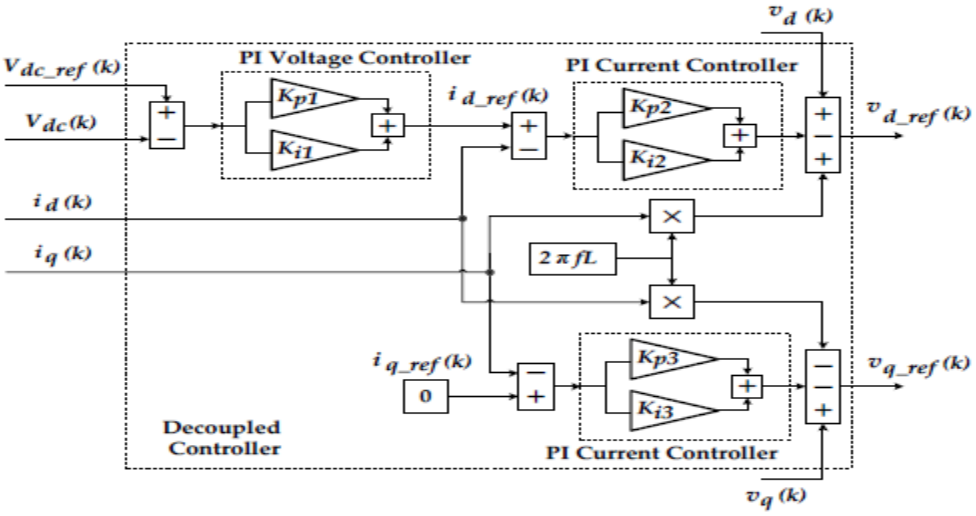

Fig.3.9 The control circuit of the decoupled controller for the voltage-oriented controller technique.

After that, the produced v_{d-ref}, v_{d-ref}in the rectifier side will be transferred to a stationary reference frame $v_{\alpha-ref}, v_{\beta-ref}$ obtained uising inverse park's transformation as equation (3.11) depicts:

$$\begin{bmatrix} v_{\alpha-ref} \\ v_{\beta-ref} \end{bmatrix} = \begin{bmatrix} \sin\theta & -\cos\theta \\ \cos\theta & \sin\theta \end{bmatrix} \begin{bmatrix} v_{d-ref} \\ v_{q-ref} \end{bmatrix} \tag{3.11}$$

At last, the switch signal S_a, S_b, S_c is generated using SVM.

As a general summary, the voltage-oriented controller consists of a voltage controller and a current controller. The current control algorithm has two independent current controllers, which will work in the positive and negative synchronous reference frames (SRF). The positive SRF is used to control the positive current component, which rotates in a clockwise direction, whereas the negative SRF is used to control the negative current component, which rotates in the opposite direction. Since the currents occur as DC values in their frame in SRF, a tracking controller does not need to be built. Due to this advantage, the PI controller is adequate to solve the problems above [4]. **Fig.3.10** summarizes the transformations involved in voltage oriented control.

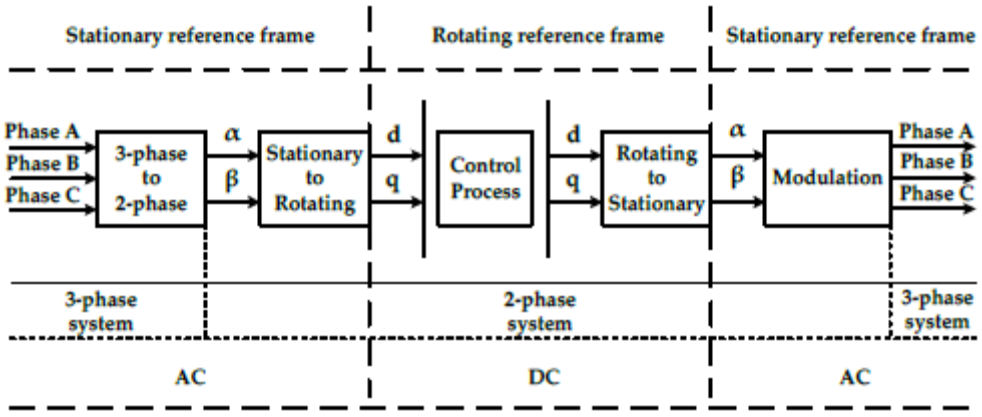

Fig.3.10 Overall domain transformation sequences involved in the voltage-oriented controller technique [5]

3.6 Simulation and results discussion

In order to verify the operation of conventional PWM rectifier and Vienna rectifier under VOC control method, their control schemes were implemented using SIMULINK. The control performances are compared beneath a step change of DC-voltage reference from 600 up to 700 at t=1s. Within the first part, the simulation is run under ideal sinusoidal grid

voltages. However, in the second part, the presented control technique is tested under distorted and unbalanced networks.

3.6.1 Part I: Ideal sinusoidal network:

3.6.1.1 Output DC-voltage

The DC-bus waveforms obtained by the simulation are shown in **fig.3.11** The overall steady state performances of the two rectifiers are nearly identical, however, their transient responses under the step change are different, Vienna's response is smoother and faster, the conventional rectifier has a higher overshoot and undershoot.

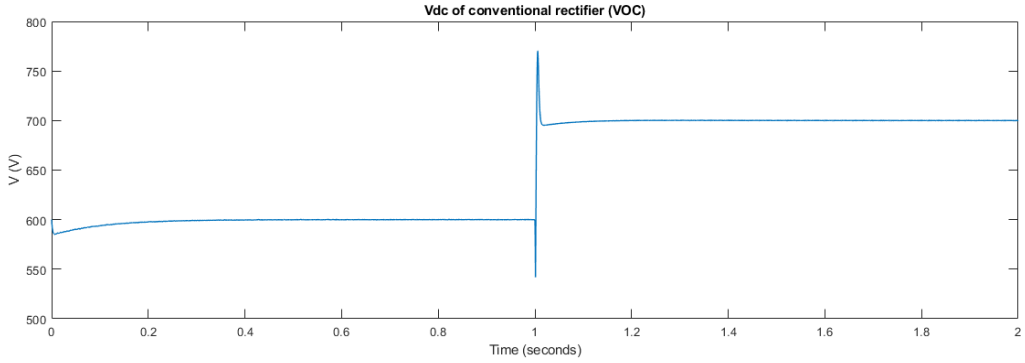

(a)

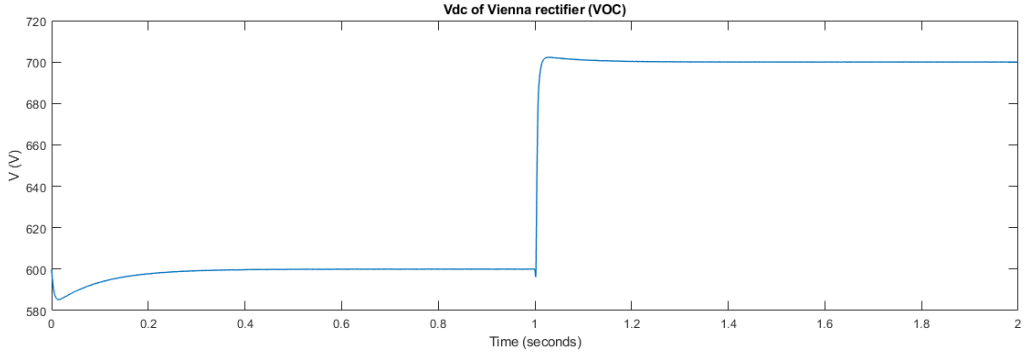

(b)

Fig.3.11 DC-bus voltage of conventional (a) and Vienna (b) rectifier using VOC control technique

3.6.1.2 Line current :

As shown in **Fig.3.12** The line current waveforms of Vienna rectifier offers lower current distortion THD=2.215%, where the conventional have the distortion THD=3.574%.

Despite these differences, the obtained line currents for the two rectifiers are sinusoidal with a sufficiently low level of harmonic distortions.

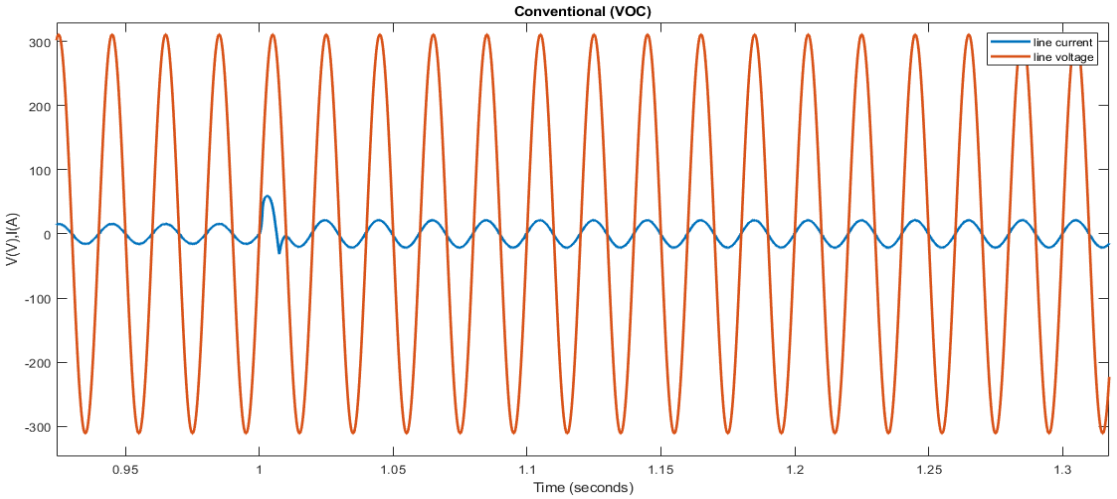

(a)

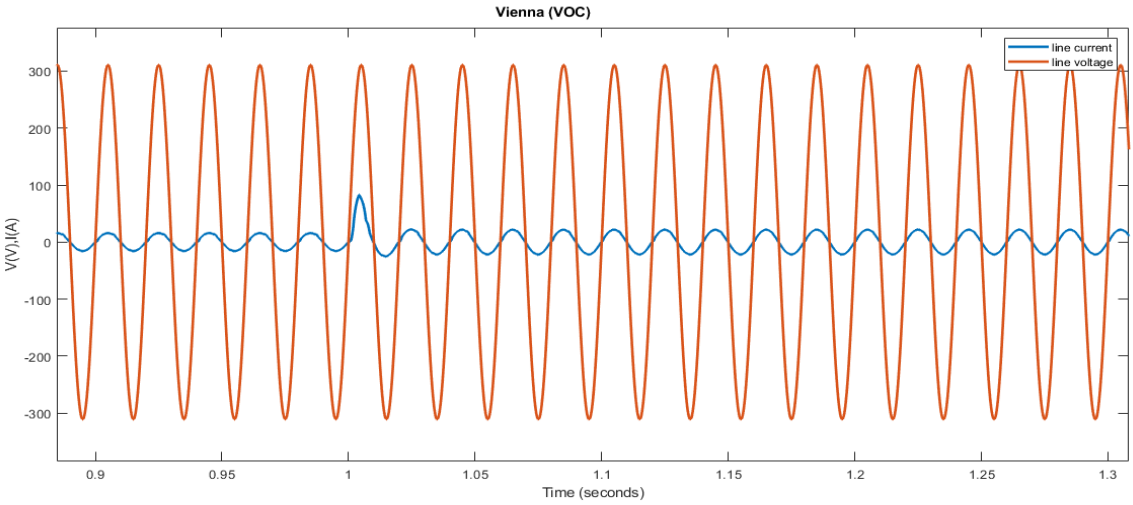

(b)

Fig.3.12 Line voltage and current of conventional (b) and Vienna (b) rectifier using VOC control technique

3.6.1.3 Active and reactive powers

From the depicted active and reactive powers waveforms of **Fig.3.13**, it can be seen that the reactive power for both rectifiers is approximately zero. The active and reactive powers of Vienna have lower ripples and overshoots and has no undershoots, while for the conventional rectifier overshoot and ripples are larger. And more importantly unity power factor requirement is successfully met.

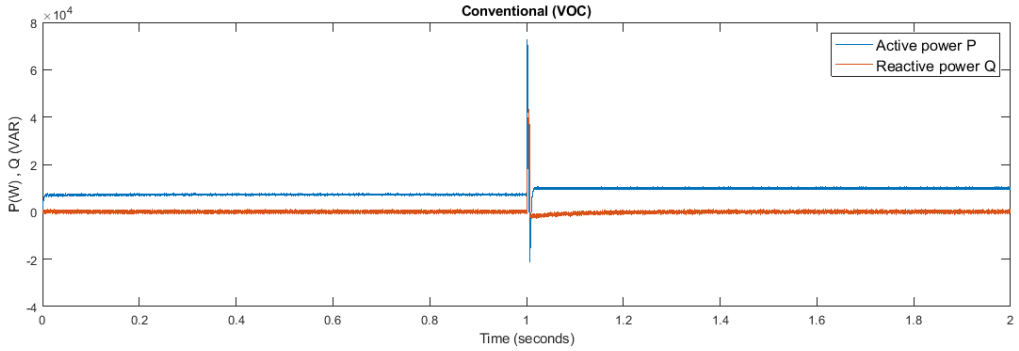

(a)

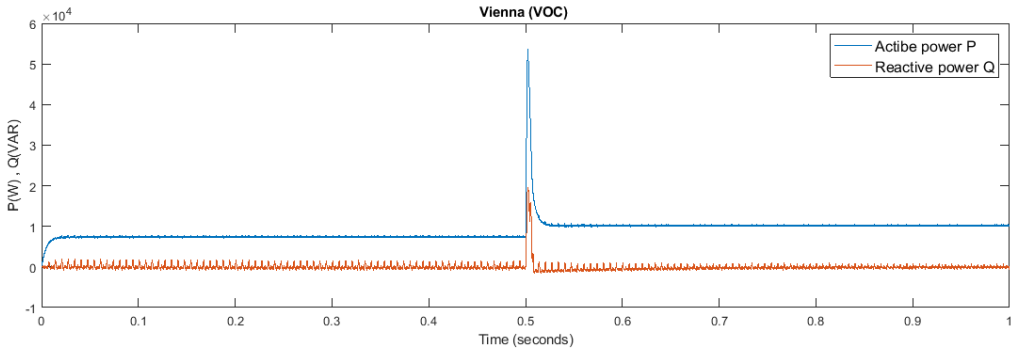

(b)

Fig.3.13 Active and reactive power of conventional (a) and Vienna (b) rectifier using VOC control technique

3.6.2 Part II: **Distorted and unbalanced networks*:***

In practical applications, it is very likely that the network might be under distortions or unbalance conditions, So, it is necessary to test and measure the harmonic distortion into the line current for both conventional and Vienna rectifier, therefore some simulations are performed in **Fig.3.14** that result total harmonic distortion given in **Table.3.2**

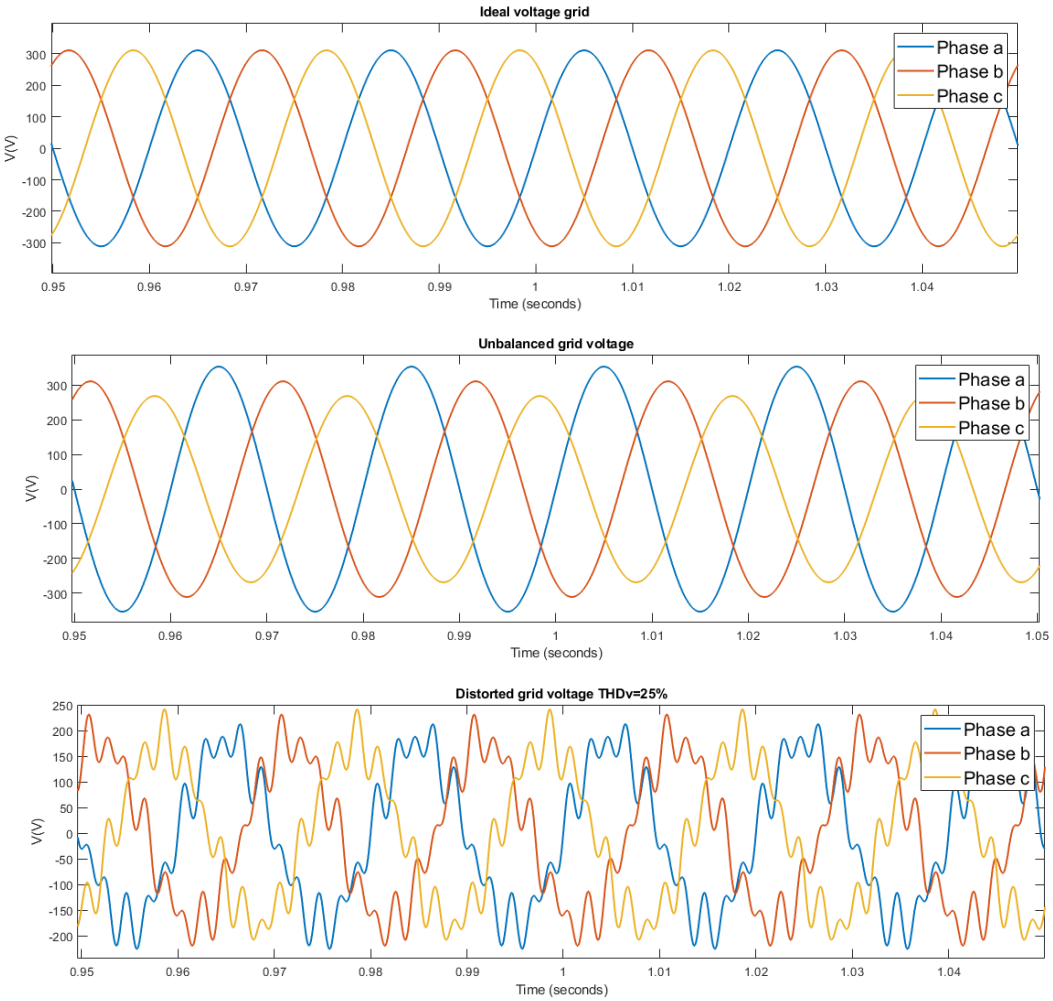

Fig.3.14 Grid voltage for ideal, distorted, and unbalanced conditions

Control technique	Ideal network	Distorted network	Unbalanced network
Conventional rectifier	3.574%	20.670%	9.114%
Vienna rectifier	2.215%	17.430%	8.596%

Table.3.2 Line current THD of conventional and Vienna rectifier using VOC control technique

The previous results show that the line current THD for both rectifiers increases under distorted network and unbalanced networks.

3.7 Comparative study

The performance of PWM and Vienna rectifiers using VOC can be summarized in the table below:

feature	PWM rectifier	Vienna rectifier
structure	Simple	complex
Switching frequency	Constant	constant
Cost of implementation	Low	lower
Computational effort	High	Very high
Output voltage	-low ripples -contain undershot and overshot -fast response	-lower ripples -does not contain any overshot or undershot -faster response
Current distortion	High	low
Grid disturbances	High THD	Low THD

Table.3.3 comparative study of PWM and Vienna rectifiers using VOC

3.8 Conclusion

In the end of this chapter, we conclude that VOC is less costly and high reliability however it is very complex due the using of decoupling blocks, two co-ordinates transform, SVM modulator and three PI controllers whose tuning largely depend on the circuit parameters. Hence VOC gives a good switching state but not the optimum. Vienna rectifier shows a better performance including: low ripples in the output DC-link, low current distortion and high power factor. the main reason for obtaining these results is because Vienna rectifier is a three level rectifier while PWM rectifier is two level rectifier.

Chapter IV

Model predictive control of PWM and VIENNA rectifiers

4.1 Introduction

This chapter is devoted to current predictive control. The predictive control is an advanced control technique which is widely used in power electronics applications due to its favorable characteristics that was achieved by the development of microprocessors. This control strategy solves issues which are faced in voltage oriented control (VOC).

The first part describes the analogy of predictive control is which is based on forecasting the optimum next switching action by discretizing the system model each sampling instant T_s. It also covers briefly features of the two types for this strategy: finite control set (FCS) which is proposed in this thesis and continuous control set (CCS). Then it will discuss the main differences of using this strategy for both PWM and Vienna rectifiers. Finally, the control schemes are simulated in SIMULINK for PWM and Vienna rectifiers to evaluate their performances under different network conditions.

4.2 Predective control

Predictive control was developed in the middle of the 1970s. It originally referred to a kind of advanced computer control algorithm that appeared in complex industrial processes [8]. Using predictive algorithms in the control of PWM rectifier that was proposed by Antoniewicz in 2008 which used Model Predictive Control (MPC) [30] Model predictive control (MPC) has become a very attractive strategy for controlling power converters. Based on the discrete model, MPC can derive the prediction of control variables for future moments within finite prediction horizon. By minimizing the cost function evaluating the difference between prediction and reference, an optimal control sequence can be obtained [31]. **Fig.4.1** shows different predictive control's classification for power electronics.

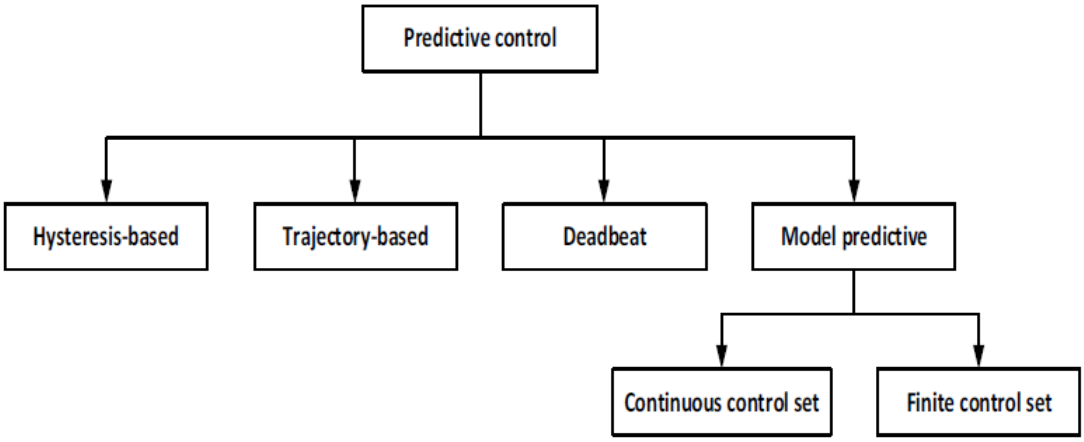

Fig.4.1 Classification of predictive control methods used in power electronics

(Cortes et al.,2008 © IEEE) [32]

In this thesis, we will introduce only model predictive which consists of two types:

MPC with finite control set: is an intuitive and easy-to-implement MPC algorithm using the switching actions as the system inputs directly. Due to the finiteness of the switching actions, FCS-MPC evaluates each switching action by applying them into the cost function. Search for the optimal control action minimizing the cost function's value [33].

MPC with continous control set: The algorithm selecting the continuous control signals as the system input is referred to as CCS-MPC. Different from FCS-MPC, CCS-MPC provides constant switching frequency. Among various CCS-MPC, optimal switching sequence (OSS) MPC strategy considers the commutation instants as the system input [31].

Table.4.1 illustrate different characteristics of two types for model predictive

MPC with finite control set	MPC with continous control set
High computations	Low computations
Doesn't require modulator	Requires modulator
Variable switching frequency	Constant switching frequency
Simple to develop & implement	More complex to derive and implement

Table 4.1 Differences between finite and continuous control set MPC [32]

4.3 Model predictive-finite state control strategy

FCS-MPC is used where the traditional PID controller is slow and the system is multiobjective and non-linear. To implement this strategy, the following steps must be taken in design stage [32]:

- Modeling the converter topology including all possible switching states.
- Defining the cost function based on the required performance.
- Discretizing the system model to predict the future state of input variables such that the cost function is optimized.

Fig.4.2 show the basic principle of predictive control for current finite control set which we are going to discuss in this thesis:

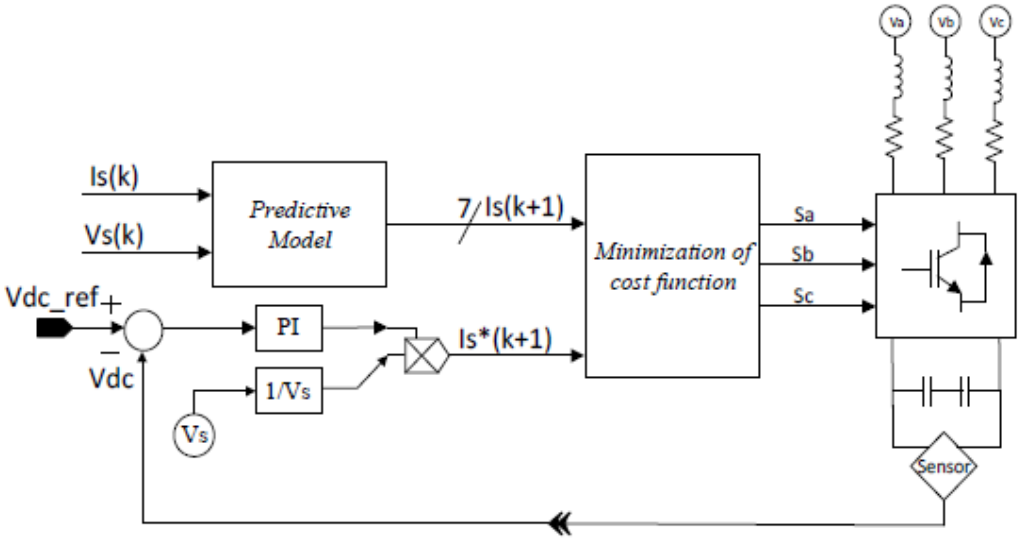

Fig.4.2 Basic principle of predictive current control [6]

4.4 Model predictive -finite state control for conventional PWM rectifier

As discussed earlier in chapter I conventional PWM rectifier can be divided into AC-side and a DC-side co-joined by a bridge converter. For defining mathematical model discretization for MPC-FCS in PWM rectifier only AC side description is needed as shown in **fig.4.3**

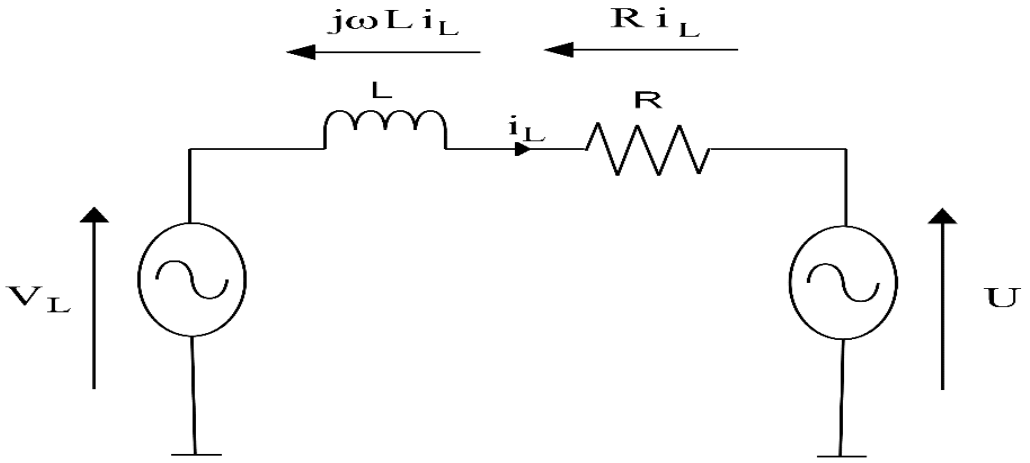

Fig.4.3 Single phase representation of the AC side of three phase PWM rectifier

Applying the KVL to derive the voltage and current equations of the rectifier in three-phase reference frame:

$$\begin{bmatrix} V_a \\ V_b \\ V_c \end{bmatrix} = R \begin{bmatrix} i_a \\ i_b \\ i_c \end{bmatrix} + L \frac{d}{dt} \begin{bmatrix} i_a \\ i_b \\ i_c \end{bmatrix} + \begin{bmatrix} U_a \\ U_b \\ U_c \end{bmatrix} \tag{4.1}$$

Equation (4.1) can be described in α, β reference :

$$L \frac{di_{\alpha\beta}}{dt} = V_{L\alpha\beta} - Ri_{\alpha\beta} - U_{\alpha\beta} \tag{4.2}$$

Derivative discretization of a continuous-time function x(t) using Euler's approximation at instant k for a sampling period T_s:

$$\left.\frac{dx(t)}{dt}\right|_{t=k} = \frac{1}{T_s}(x(k+1) - x(k) \tag{4.3}$$

Replacing (4.3) in (4.2) yields:

$$i_{\alpha\beta}(k+1) = \left(1 - \frac{RT_S}{L}\right) i_{\alpha\beta}(k) + \frac{T_S}{L}\left(V_{L\alpha\beta}(k) - U_{\alpha\beta}(k)\right) \tag{4.4}$$

Where

$$U_\alpha(k) = S_\alpha V_{dc}(k) = \sqrt{\frac{2}{3}}\, V_{dc}(k)\left(S_a - \frac{1}{2}(S_b + S_c)\right) \tag{4.5a}$$

$$U_\beta(k) = S_\beta V_{dc}(k) = \sqrt{\frac{1}{2}}\, V_{dc}(k)(S_b - S_c) \tag{4.5b}$$

V_k	S_a	S_b	S_c	U_α/V_{dc}	U_β/V_{dc}
V_0	0	0	0	0	0
V_1	1	0	0	1	0
V_2	1	1	0	$1/2$	1
V_3	0	1	0	$-1/2$	1
V_4	0	1	1	-1	0
V_5	0	0	1	$-1/2$	-1
V_6	1	0	1	$1/2$	-1
V_7	1	1	1	0	0

Table 4.2 Converter voltage for different switching states

Where the bridge converter voltage denoted 'V_k'. when the behavior of i_α and $i_\beta$is approximated for the future instant (k+1) . Then the control target is to minimize the error between the reference currents $i_\alpha^*$and i_β^* using cost function that is described in equation (4.6):

$$CF = (i_\alpha^* - i_\alpha(k+1))^2 + (i_\beta^* - i_\beta(k+1))^2 \quad (4.6)$$

Both $i_\alpha^*$and $i_\beta^*$are obtained by the DC voltage control loop.

It should be noted that the active vector should be followed by an appropriate zero vector with minimal switching jumps. For vectors (110, 011, 101), they should be followed by (111), while for other vectors (100, 010, 001), they should be followed by (000). Hence, no more than one commutation event occurs simultaneously during one control period [7].

4.5 Model predective control-finite state control for vienna rectifier PWM

4.5.1 Mathematical model discretization

This approach is introduced in details on paper [10]

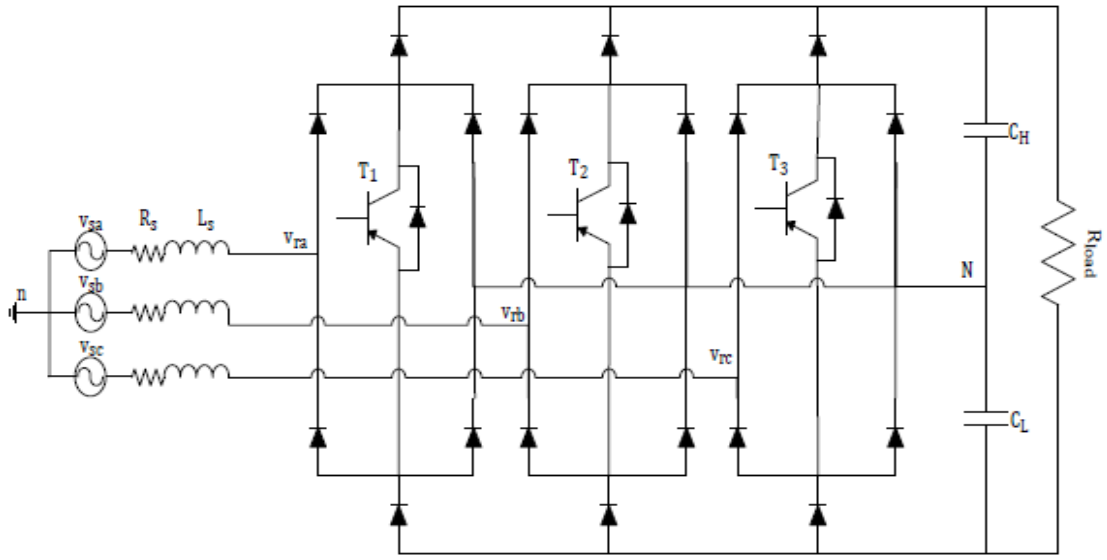

Fig.4.4 Vienna rectifier topology

Applying KVL law on rectifier pole in **fig.4.4**

$$V_{Sabc} = L_s \frac{di_{Sabc}}{dt} + R_S i_{abc} + v_{rabcN} - v_{Nn} \tag{4.7}$$

Writing equation (4.7) in vector form yields:

$$\overrightarrow{V_S} = L_S \frac{d}{dt}\left(\overrightarrow{I_S}\right) + R_S\left(\overrightarrow{I_S}\right) + \overrightarrow{V_{rN}} - \overrightarrow{V_{Nn}} \tag{4.8}$$

(Where $V_{rN}$is rectifier switching voltage and defined as:$V_{rN} = K_r * \frac{V_{DC}}{2}$ where K_r is the switching function that have already been disscused earlier.

Applying Euler forward method we get:

$$\overrightarrow{I_S}(k+1) = \frac{T_S}{L_S}\left[\overrightarrow{V_S}(k) - \overrightarrow{V_{rN}}\right] + (1 - \frac{R_S T_S}{L_S})\overrightarrow{I_S}(k) \tag{4.9}$$

Applying all seven feasible vectors for the next sampling interval we obtain all seven predicted currents in $\alpha\beta$ coordinates:

$$\mathrm{i_{s\alpha\beta}(k+1)} = \frac{\mathrm{T_S}}{\mathrm{L_S}}\left[\mathrm{v_{s\alpha\beta}(k)} - \mathrm{K_{\alpha\beta}} * \frac{\mathrm{V_{DC}}}{2}\right] + \left(1 - \frac{\mathrm{R_S T_S}}{\mathrm{L_S}}\right)\mathrm{i_{s\alpha\beta}(k)} \tag{4.10}$$

Where K_α and K_β are the resultant clarke's transformation of the switching function as illustrated below:

$$\begin{bmatrix} K_\alpha \\ K_\beta \end{bmatrix} = \frac{2}{3}\begin{bmatrix} 1 & -\frac{1}{2} & \frac{1}{2} \\ 0 & \frac{\sqrt{3}}{2} & -\frac{\sqrt{3}}{2} \end{bmatrix}\begin{bmatrix} K_a \\ K_b \\ K_c \end{bmatrix} \quad (4.11)$$

It is noticed that equation (4.11) is affected by both the polarity of currents and switching state.The following set of tables shows different values for K_α and K_β in sector 1 and sector 4

vector	S_A	S_B	S_C	K_A	K_B	K_C	K_α	K_β
V_2	0	0	0	+1	-1	-1	$4/3$	0
V_{18}	0	0	1	+1	-1	0	1	$-\sqrt{3}/3$
V_3	0	1	0	+1	0	-1	1	$\sqrt{3}/3$
V_1	0	1	1	+1	0	0	$2/3$	0
V_1	1	0	0	0	-1	-1	$2/3$	0
V_{16}	1	0	1	0	-1	0	$1/3$	$-\sqrt{3}/3$
V_4	1	1	0	0	0	-1	$1/3$	$\sqrt{3}/3$
V_{19}	1	1	1	0	0	0	0	0

Table 4.3 switching states and corresponding vectors in sector 1 [6]

vector	S_A	S_B	S_C	K_A	K_B	K_C	K_α	K_β
V_{11}	0	0	0	-1	+1	+1	$-4/3$	0
V_9	0	0	1	-1	+1	0	-1	$\sqrt{3}/3$
V_{12}	0	1	0	-1	0	+1	-1	$-\sqrt{3}/3$
V_{10}	0	1	1	-1	0	0	$-2/3$	0
V_{10}	1	0	0	0	+1	+1	$-2/3$	0
V_7	1	0	1	0	+1	0	$-1/3$	$\sqrt{3}/3$
V_{13}	1	1	0	0	0	+1	$-1/3$	$-\sqrt{3}/3$
V_{19}	1	1	1	0	0	0	0	0

Table 4.4 switching states and corresponding vectors in sector 4

It is noticed that in both sector (1) and sector (4) there are repeated values of K_α,K_β for switching state 011 and 100 respectively.in order to guarantee no more than one commutation event occurs simultaneously during one control period. We check the previous switching state for vectors (111, 001, 010), they should be followed by (011), while for other vectors (000, 101, 110), they should be followed by (100). In sector (2) and (5) the repeated values of K_α, K_β for switching state 001 and 110 respectively. We check the previous switching state for vectors (000, 011, 101), they should be followed by (001), while for other vectors (010, 100, 111), they should be followed by (110). In sector (3) and (6) the repeated values of K_α for switching state 010 and 101 respectively. We check the previous switching state for vectors (000, 011, 110), they should be followed by (010), while for other vectors (001, 100, 111), they should be followed by (101).

Finally, the control target is to minimize the error between the reference currents i_α^*, i_β^* and predicted current using cost function that is described in equation(4.12):

$$CF = (i_{s\alpha}^* - i_{s\alpha}(k+1))^2 + (i_{s\beta}^* - i_{s\beta}(k+1))^2 \qquad (4.12)$$

4.5.2 Implantation strategy of current MPC-FCS in Vienna rectifier

As it has been seen earlier in section (4.3.1) the mathematical discretization for MPC-FCS is strongly depending on both current polarity and switching state. In order to distinguish the polarity of each sector. It can be done by a simple comparator in order to compare the sign of three phase current continuously.

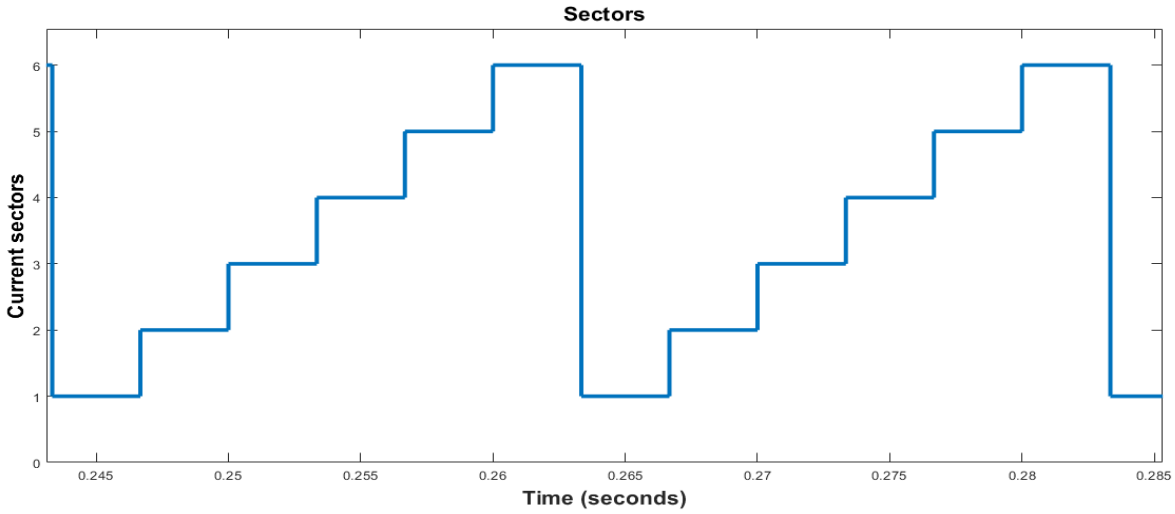

Fig.4.5 Current sectors

After that the cost function is optimized by evaluating all eight feasible vector in each sector in order to achieve smallest possible minimum error between the reference current $i_{\alpha}^{*}$and i_{β}^{*} and the target contol current. Where $i_{\alpha}^{*}$and $i_{\beta}^{*}$are obtained by the DC voltage control loop. As illustrated in **fig.4.6**:

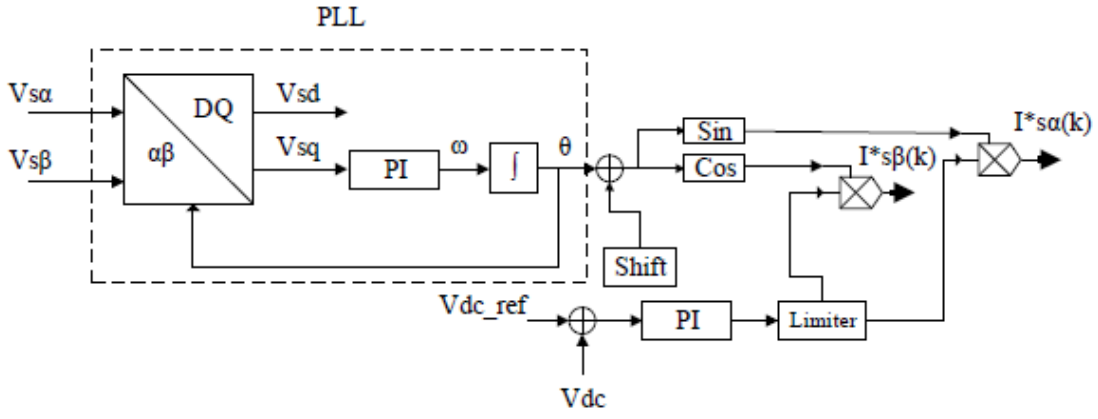

Fig4.6 Block diagram for generating current reference [6]

4.6 Simulation and comparission study

To implement the control schemes of PWM and Vienna rectifier under Finite control set model predictive control method, SIMULINK is used. Like previous simulations, the control performances are compared under a step change of DC-voltage reference from 600 up to 700 at t=1s. firstly the simulation is run under ideal sinusoidal grid voltages, then, the FCS_MPC control technique is tested under distorted and unbalanced networks.

4.6.1 Part I: Ideal sinusoidal network:

4.6.1.1 Output DC-voltage

The DC-bus waveforms obtained by the simulation are shown in **fig.4.7** The overall steady state performances of the two rectifiers are nearly identical, however, their transient responses are different, the conventional rectifier has a higher overshoot and undershoot. However, Vienna's response is smoother and faster.

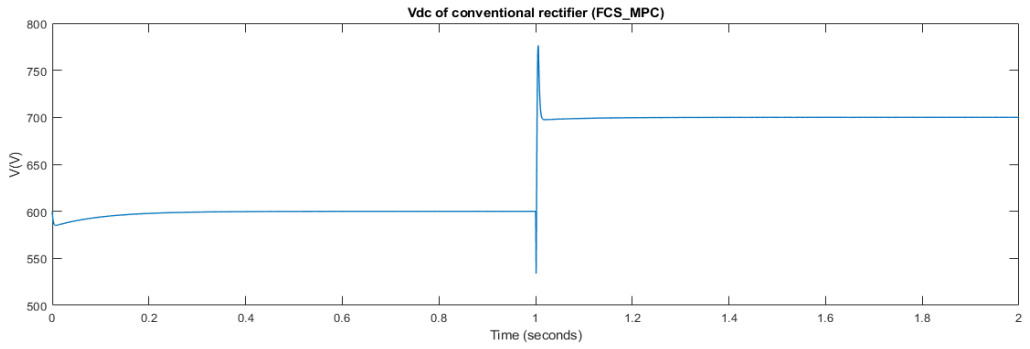

(a)

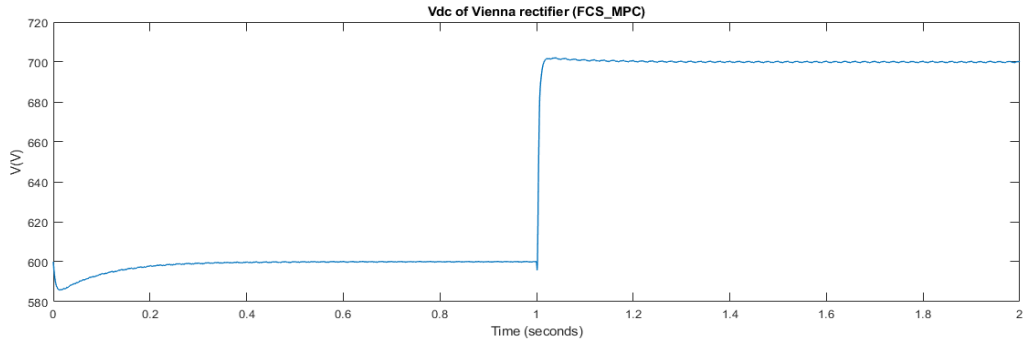

(b)

Fig.4.7 DC-bus voltage of conventional (a) and Vienna (b) rectifier using FCS_MPC control technique

4.6.1.2 Line current:

The line current waveforms of Vienna rectifier has lower current distortion THD=0.9707% As shown in **Fig.4.8**, where PWM rectifier has the distortion THD=1.6340%. However, the obtained line currents for the two rectifiers are sinusoidal with a sufficiently low level of harmonic distortions.

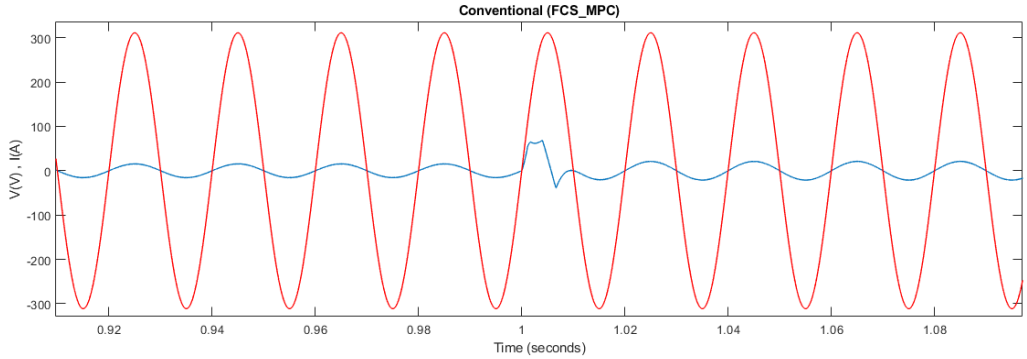

(a)

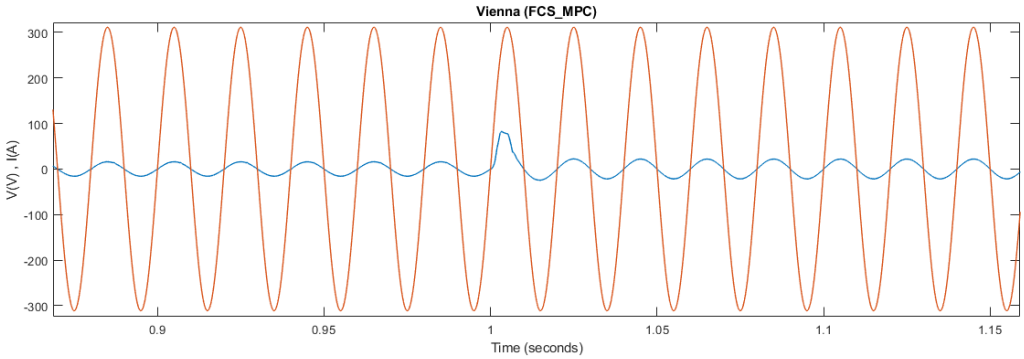

(b)

Fig.4.8 Line voltage and current of conventional (a) and Vienna (b) rectifier using FCS_MPC control technique

4.6.1.3 Active and reactive powers

From the active and reactive powers waveforms shown below, it can be seen that the reactive power for both rectifiers is approximately zero. The active and reactive powers of Vienna have higher ripples and lower overshoots and have no undershoots, while for the conventional rectifier overshoots are larger. And most importantly unity power factor requirement is successfully met.

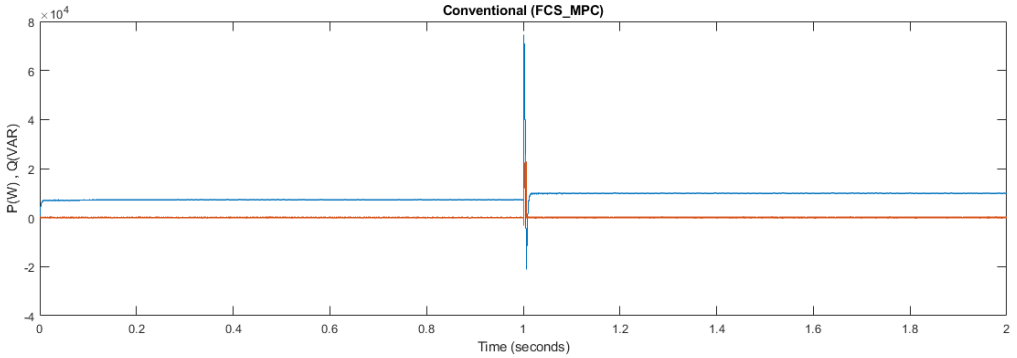

(a)

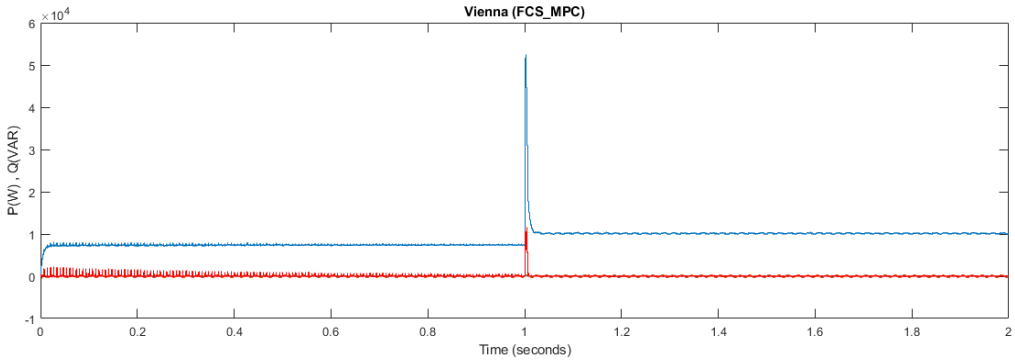

(b)

Fig.4.9 Active and reactive power of conventional (a) and Vienna (b) rectifier using FCS_MPC control technique

4.6.2 Part II: Distorted and unbalanced networks*:*

After testing and measuring the harmonic distortion into the line current for both conventional and Vienna rectifier using simulations depicted in **Fig.4.10**. the results of total harmonic distortion are given in **Table.4.5.**

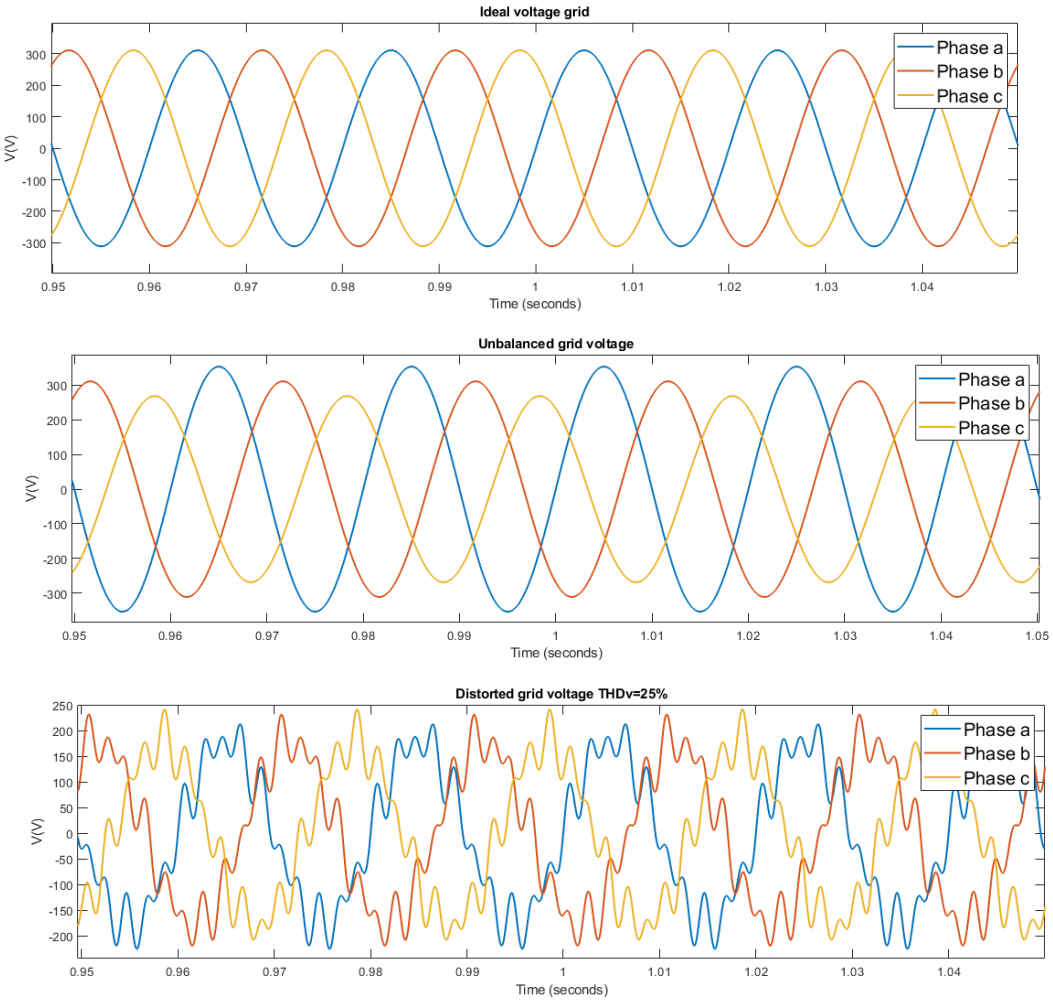

Fig.4.10 Grid voltage for ideal, distorted, and unbalanced conditions

Control technique	Ideal network	Distorted network	Unbalanced network
Conventional rectifier	1.6340%	26.23%	8.50%
Vienna rectifier	0.9707%	16.81%	8.224%

Table.4.5 Line current THD of conventional and Vienna rectifier using VOC control technique

The previous results show that the line current THD for both rectifiers increases under distorted network and unbalanced networks.

4.7 Comparative study

The performance of PWM and Vienna rectifiers using current predictive control- finite control set can be summarized in the table below:

feature	PWM rectifier	Vienna rectifier
structure	Simple	Complex
Switching frequency	Variable	Variable
Computational effort	-high -discretized model system depends only on the switching state.	-Very high -discretized model system depends on the switching state and line-currents polarity.
Output voltage	-low ripples -contain undershot and overshot in the transient response -fast response	-low ripples -does not contain any overshot or undershot in the transient response -faster response
Current distortion	High	low
Grid disturbances	High THD	Low THD

Table.4.6 Comparative study of PWM and Vienna rectifiers using VOC

4.8 Conclusion

In the end of this chapter, we can conclude that predictive control- finite control set is much simpler than VOC. Using this strategy allow to achieve optimum switching state however it operates with a variable switching state. It less affected by the PI tuning compared to voltage oriented control. Discretizing the system model to predict the future state of input variables give seven possible switching state for PWM rectifier while there are fourty eight possible switching state since its operation highly in currents line polarity. Vienna rectifier shows a better performance including: low ripples in the output DC-link and low current distortion under balanced, unbalanced distorted network however PWM has a better power factor.

General conclusion and future perspective

General conclusion

The purpose of the presented thesis is to compare of the performance of PWM and Vienna rectifiers using VOC and current MPC -FCS under variant conditions. The criterion is well satisfied: high power factor, low ripple factor, low harmonics distortion. Vienna rectifier shows a better performance than PWM rectifier.

Although VOC is less costly, operating with constant switching frequency. However, it is too complex since it uses decoupling blocks, co-ordinate transformation and SVM modulator. In this Vienna rectifier shows a better performance especially for low ripple DC-voltage. The DC-bus waveforms is very smooth, the transient response under step change is faster. Moreover, it has no overshot and undershot.

In the last chapter, Current MPC-FCS which is much simpler than VOC. It is based on discretizing the system model to predict the future state of the input variable such that the cost function is optimized. It uses no SVM modulator but it operates with variable switching frequency. Both PWM and Vienna rectifiers show a better performance than VOC.

Finally, it can be concluded that Vienna rectifier is more reliable, has better performance hence it is more suitable for different AC/DC conversion. However, the performance is highly affected by the tuning of PI controller.

Future prospective

Future work on Vienna rectifier could be oriented towards the following:

- Perform the experimental implementation of the proposed control strategies.
- Evaluate the performance of Vienna rectifier using advanced control Model predictive control.
- Application of sensorless control using virtual flux principle.
- Solving the problem of tuning in PI controller using more advanced controllers like fuzzy logic control.
- Apply the proposed control strategies for electric vehicle charging stations.

Appendices

Appendix A: Park and Clarke transformation

Clarke and Park transformations are used in high performance architectures in three phase power system analysis. Current and voltage are represented in terms of space vector which is represented in a stationary reference frame. A general rotating reference frame has then been introduced. This frame is described by d and q axes. Through the use of the Clarke transformation, the real and imaginary currents can be identified. The Park transformation is used to realize the transformation of those real and imaginary currents from the stationary to the rotating reference frame [34].

A.1 Clarke transformation:

it is common practice to transform system state variables from the three-phase system (a,b,c) to an orthogonal (α, β) representation where the resultant f denotes either the stator voltage, current or magnetic flux linkage [35].

$$\begin{bmatrix} f_\alpha \\ f_\beta \end{bmatrix} = \frac{2}{3} \begin{bmatrix} 1 & \frac{-1}{2} & \frac{-1}{2} \\ 0 & \frac{\sqrt{3}}{2} & -\frac{\sqrt{3}}{2} \end{bmatrix} \begin{bmatrix} f_a \\ f_b \\ f_c \end{bmatrix} \tag{A.1}$$

$$\begin{bmatrix} f_\alpha \\ f_\beta \end{bmatrix} = [clarke\ matrix] \begin{bmatrix} f_a \\ f_b \\ f_c \end{bmatrix} \tag{A.2}$$

It is evident from **Fig.A.1** the resultant quantity from representation (α, β) is:

$$f = \sqrt{{f_\alpha}^2 + {f_\beta}^2} \tag{A.3}$$

A.2 Park transformation:

The Park transformation has been widely used in the analysis of synchronous and induction machines. The novelty of *Park's* work involves his ability to transform any related

machine's equation set from time-varying coefficients to another with time-invariant coefficients [35]:

$$\begin{bmatrix} f_d \\ f_q \end{bmatrix} = \begin{bmatrix} \cos(\theta_r) & \sin(\theta_r) \\ -\sin(\theta_r) & \cos(\theta_r) \end{bmatrix} \begin{bmatrix} f_\alpha \\ f_\beta \end{bmatrix} \tag{A.4}$$

$$\begin{bmatrix} f_d \\ f_q \end{bmatrix} = [park\ matrix] \begin{bmatrix} f_\alpha \\ f_\beta \end{bmatrix} \tag{A.5}$$

Transformation from (α, β) to (d, q) can be done:

$$\begin{bmatrix} f_\alpha \\ f_\beta \end{bmatrix} = \begin{bmatrix} \cos(\theta_r) & -\sin(\theta_r) \\ \sin(\theta_r) & \cos(\theta_r) \end{bmatrix} \begin{bmatrix} f_d \\ f_q \end{bmatrix} \tag{A.6}$$

From equation ( ) and ( ). It can be deduced that:

$$\begin{bmatrix} f_d \\ f_q \end{bmatrix} = \frac{2}{3} \begin{bmatrix} \cos(\theta_r) & \cos(\theta_r - \frac{2\pi}{3}) & \cos(\theta_r - \frac{4\pi}{3}) \\ -\sin(\theta_r) & -\sin(\theta_r - \frac{2\pi}{3}) & -\sin(\theta_r - \frac{4\pi}{3}) \end{bmatrix} \begin{bmatrix} f_a \\ f_b \\ f_c \end{bmatrix} \tag{A.7}$$

$$\begin{bmatrix} f_d \\ f_q \end{bmatrix} = [park\ matrix][clarke\ matrix] \begin{bmatrix} f_a \\ f_b \\ f_c \end{bmatrix} \tag{A.8}$$

It is evident from **Fig.A.1** the resultant quantity from representation (d, q) is:

$$f = \sqrt{{f_d}^2 + {f_q}^2} \tag{A.9}$$

The two phases (α, β) frame representation calculated with the *Clarke* transform is then fed to a vector rotation block where it is rotated over an angle $\theta r$to follow the (d, q)reference frame attached to the rotor quantity [35]

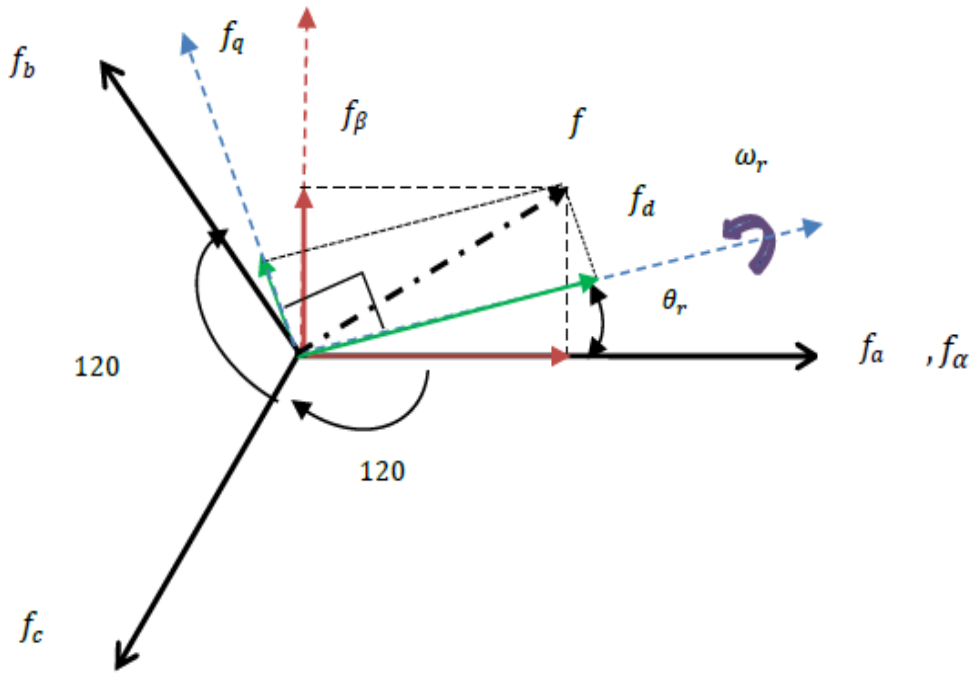

Fig.A.1: Combined stationary and rotating frames for three - phase system

Appendix B: Vienna rectifier topologies

Three variants of Vienna rectifier can be arrived at depending on how the AC switching element is realized. This results in variation in efficiency and rating of the

components used for a specified power, input voltage, and switching frequency. By replacing the AC switching element with different semiconductor combination, three different variants of the VIENNA rectifier could be realized. The schematic of the three variants of the switching element is shown in **Fig.B.1**[36]

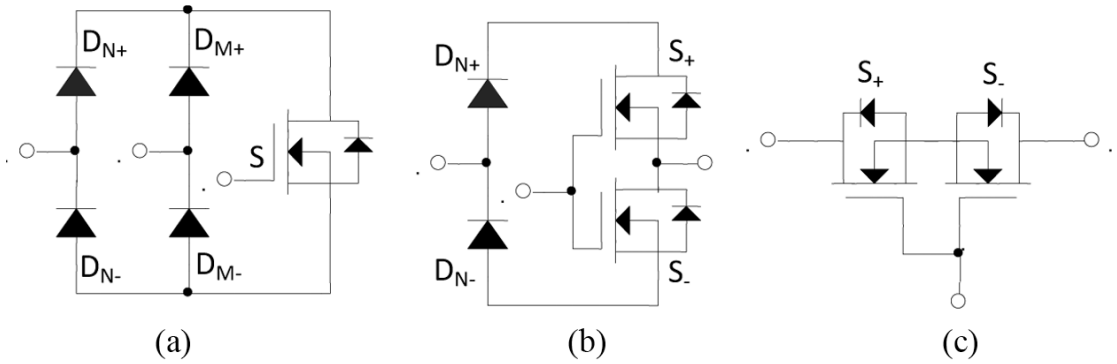

Fig.B.1: variants of AC switching elements

B.1 Topology 1:

The circuit diagram of topology 1 is illustrated in **Fig.B.2** and is realized by using the first AC switching element of **Fig.B.1 (a)**. The current passing diode D_N and D_M is a continuous 50 Hz fundamental frequency half cycle. The voltage across the diode D_N is a high frequency switching when the current is zero. Thus a low frequency diode can be used for both D_N and D_M. However, a high frequency diode is needed for D_F

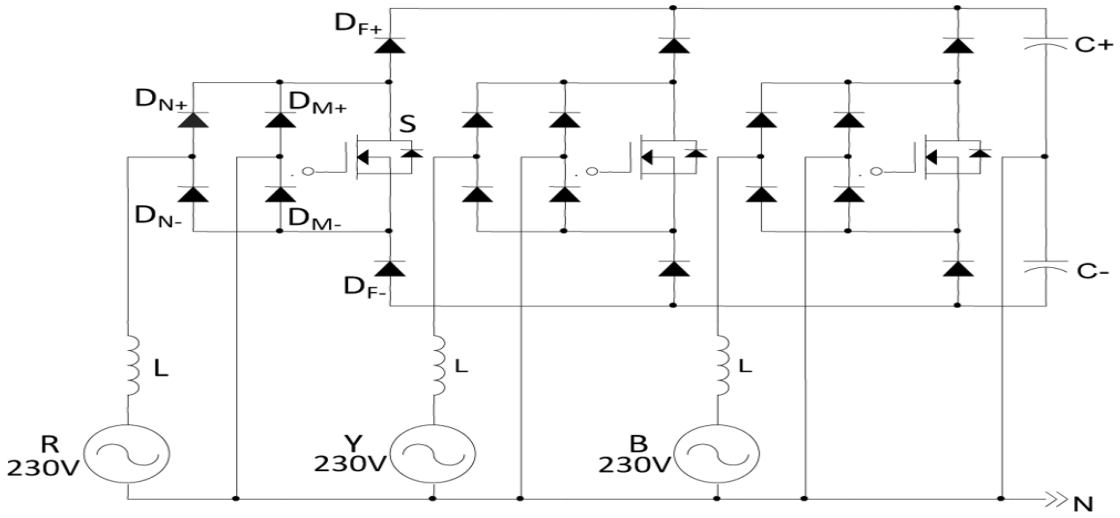

Fig.B.2: circuit diagram of topology 1 [36]

Diode D_N average and RMS current:

$$I_{DN,avg} = \frac{1}{\pi} I_N \tag{B.1}$$

$$I_{DN,rms} = \frac{1}{2} I_N \tag{B.2}$$

Where I_N is the peak line current

Diodes D_M, D_F average and RMS current:

$$I_{DM,avg} = \left(\frac{1}{\pi} - \frac{1}{2\sqrt{3}M}\right) I_N \tag{B.3}$$

$$I_{DM,rms} = \sqrt{\frac{1}{4} - \frac{4}{3\sqrt{3}\pi}\frac{1}{M}} I_N \tag{B.4}$$

$$I_{DF,avg} = \frac{1}{2\sqrt{3}M} I_N \tag{B.5}$$

$$I_{DF,rms} = \sqrt{\frac{4}{3\sqrt{3}\pi}\frac{1}{M}} I_N \tag{B.6}$$

M is the voltage transformation ratio. It is defined as:

$$M = \frac{U_0}{\sqrt{3}U_N} \tag{B.7}$$

Where U_0 is the DC output voltage and U_N is the peak phase voltage.

MOSFET average and RMS current:

$$I_{S,avg} = \left(\frac{2}{\pi} - \frac{1}{\sqrt{3}M}\right) I_N \tag{B.8}$$

$$I_{S,RMS} = \left(\frac{1}{2} - \frac{8}{3\sqrt{3}\pi M}\right)^{1/2} I_N \tag{B.9}$$

B.2 Topology 2:

The circuit diagram of topology 1 is illustrated in **Fig.B.3** and is realized by using the first AC switching element of **Fig.B.1 (b)**. The freewheeling diode current on D_F, D_N and the capacitor ripple current I_C remains the same as of topology 1, while the MOSFET current is distributed into two MOSFETs.

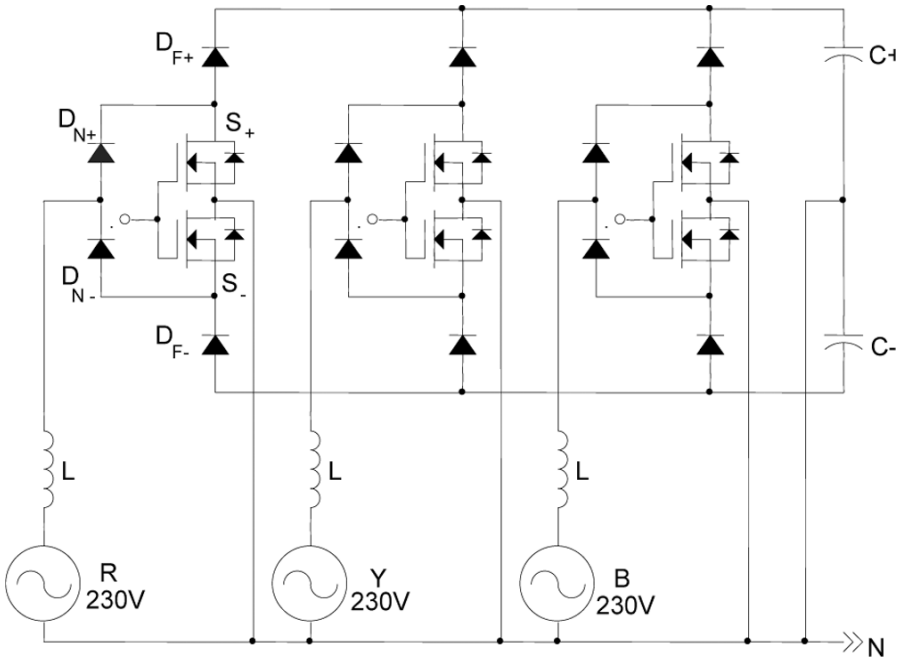

Fig.B.3: circuit diagram of topology 2 [36]

Switch S_i average and RMS current:

$$I_{S,avg} = \left(\frac{1}{\pi} - \frac{1}{2\sqrt{3}M}\right) I_N \tag{B.10}$$

$$I_{S,RMS} = \left(\frac{1}{4} - \frac{4}{3\sqrt{3}\pi M}\right)^{1/2} I_N \tag{B.11}$$

B.3 Topology 3:

The circuit diagram of topology 1 is illustrated in **Fig.B.4** and is realized by using the first AC switching element of **Fig.B.1 (c)**. The freewheeling diode current

remain same as topology 1 and 2. Whereas, the switch current when considered as a single unit, the average value is zero because of the symmetry in the current waveform, while RMS value is same as topology 1. As the switch is made up of two MOSFETs, the average and RMS current of one MOSFET will be same as topology 2. During positive half wave MOSFET S+ and the diode of S- conduct while during negative half wave MOSFET S- and the diode of S+ conduct

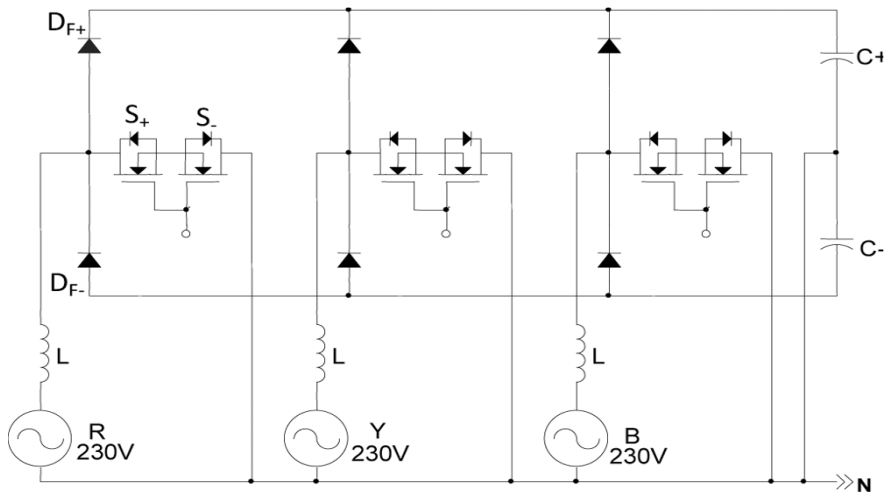

Fig.B.3: circuit diagram of topology 3 [36]

Switch S_i average and RMS current:

$$I_{S,avg} = \left(\frac{1}{\pi} - \frac{1}{2\sqrt{3}M}\right) I_N \tag{B.12}$$

$$I_{S,RMS} = \left(\frac{1}{4} - \frac{4}{3\sqrt{3}\pi M}\right)^{1/2} I_N \tag{B.13}$$

Appendix C: Simulation circuits

C.1 Voltage-oriented control (VOC):

C.1.2 Conventional rectifier:

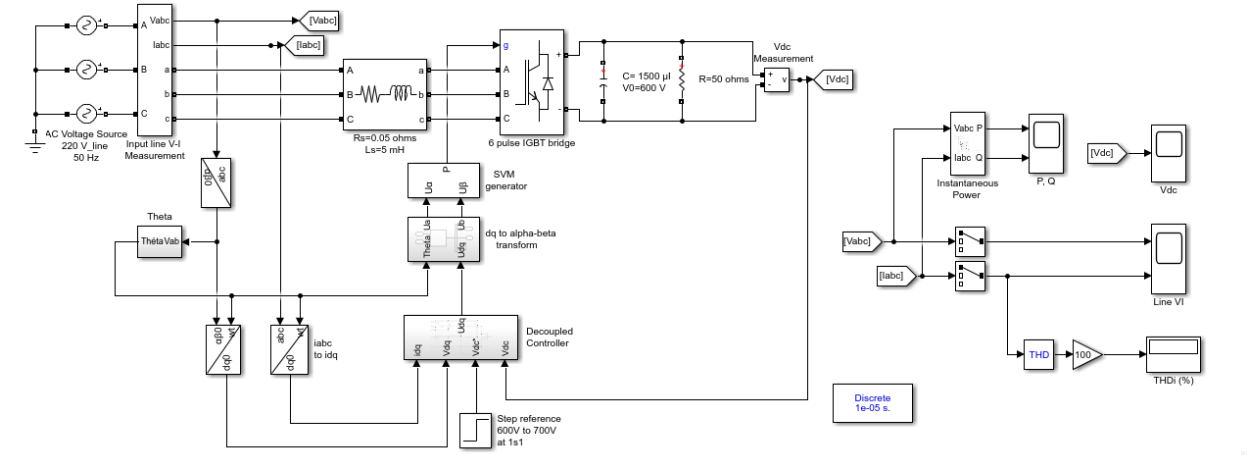

Fig.C.1 Simulation circuit of conventional rectifier with VOC.

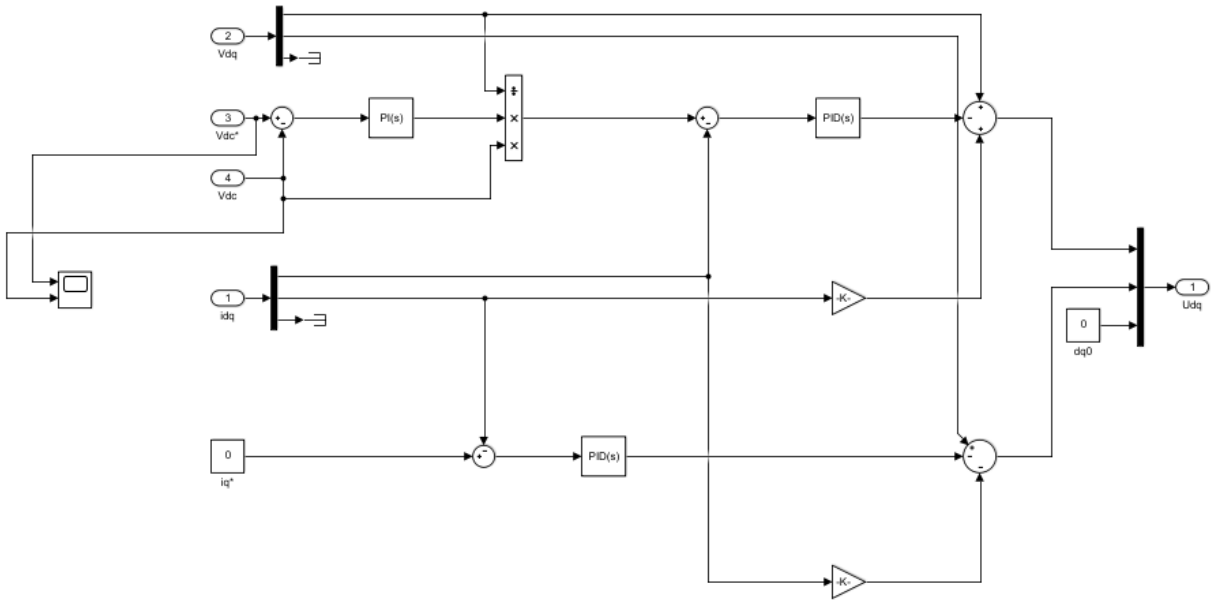

Fig.C.2 Decoupled controller block

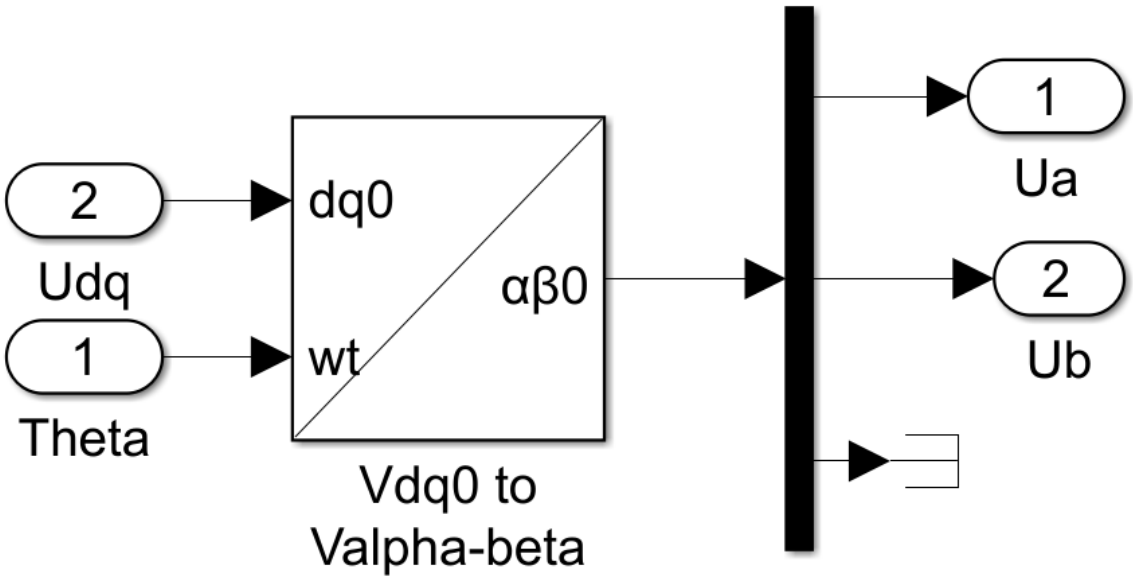

Fig.C.3 Theta to alpha-beta transform block

C.1.2 Vienna rectifier:

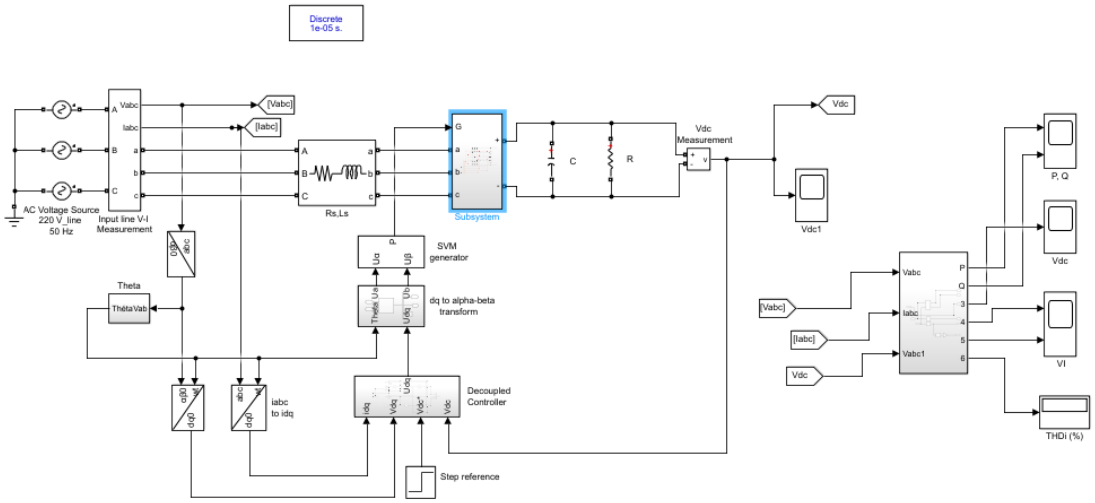

Fig.C.4 Simulation circuit of Vienna rectifier with VOC.

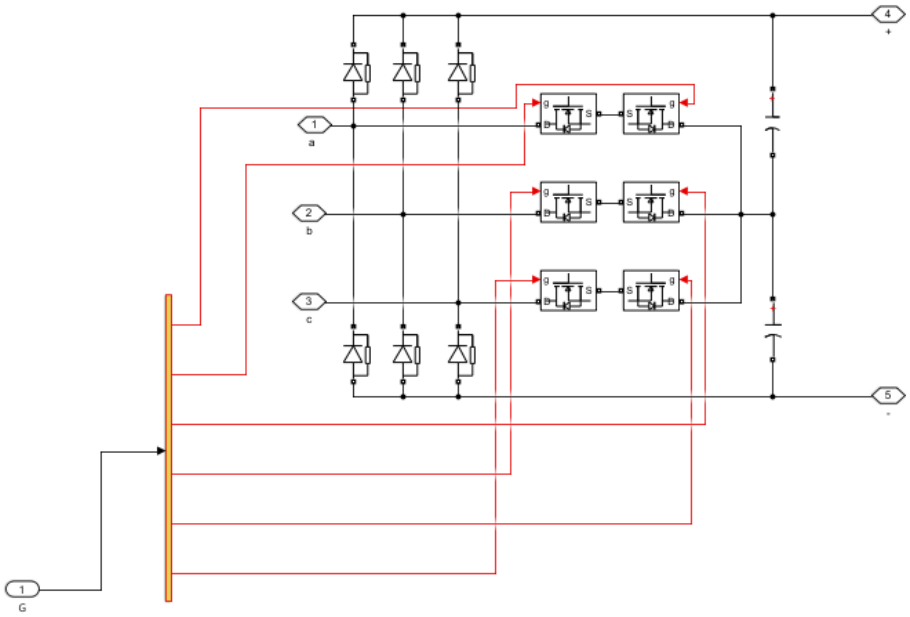

Fig.C.5 Vienna rectifier.

C.2 Finite Control Set Model Predictive Control (FCS-MPC):

C.2.1 Conventional rectifier:

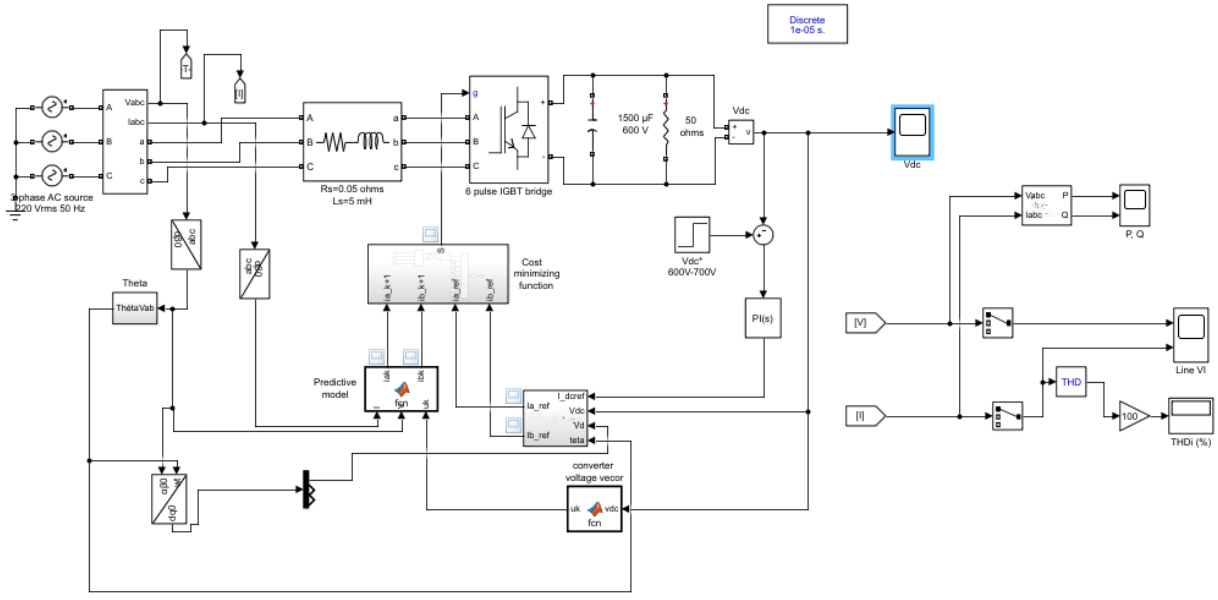

Fig.C.6 Schematic of the overall system for conventional rectifier with FCS-MPC

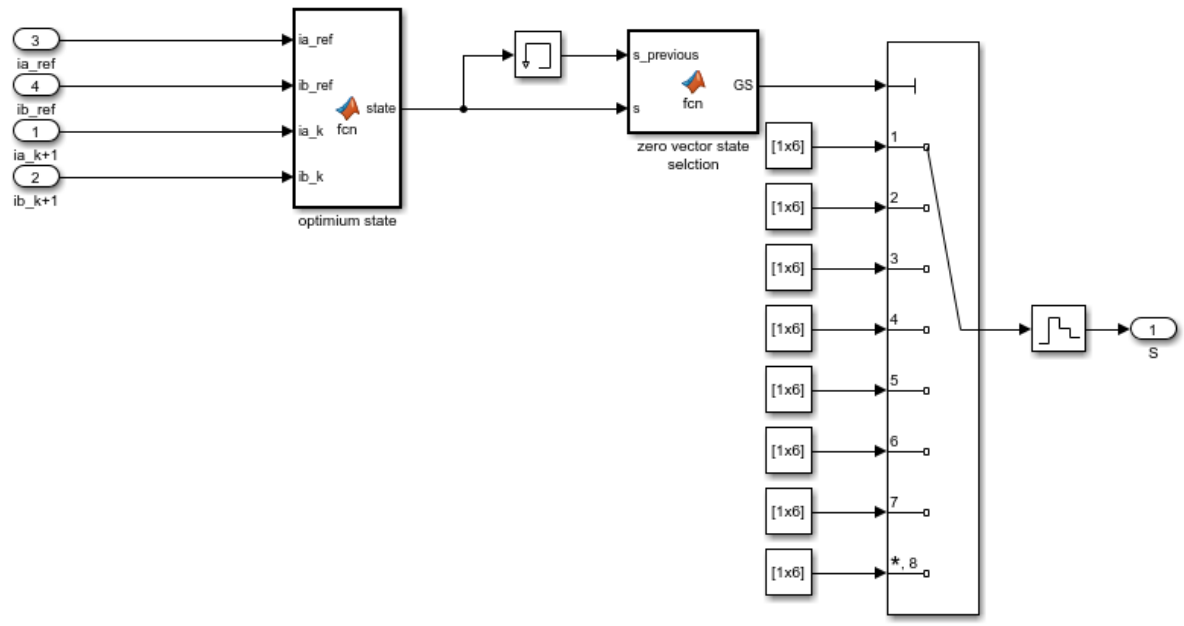

Fig.C. 7 Cost minimizing function block

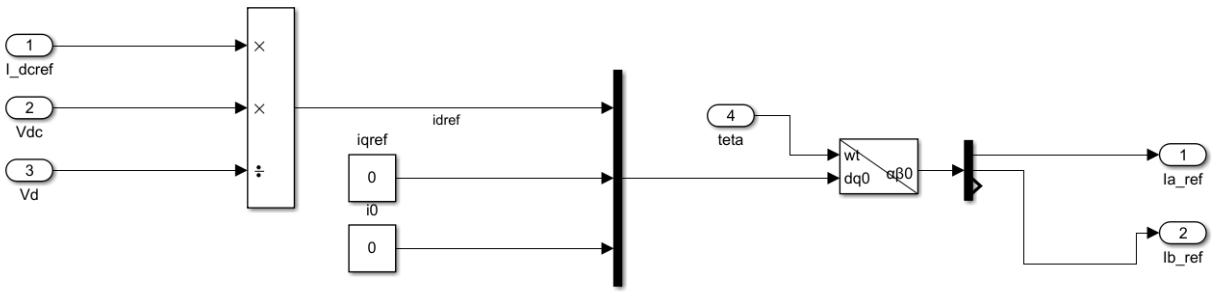

Fig.C.8 Referrence current block

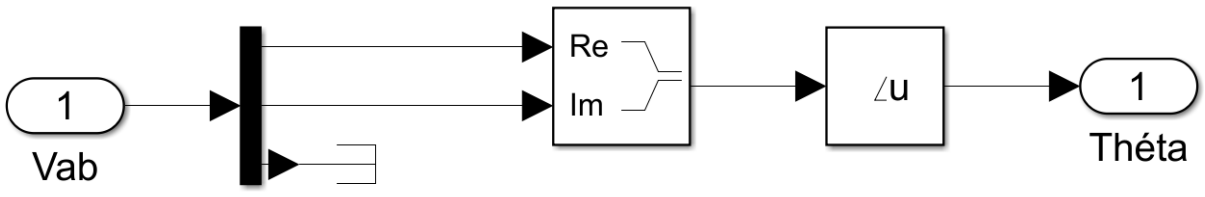

Fig.C.9 Theta block

C.2.2 Vienna rectifier:

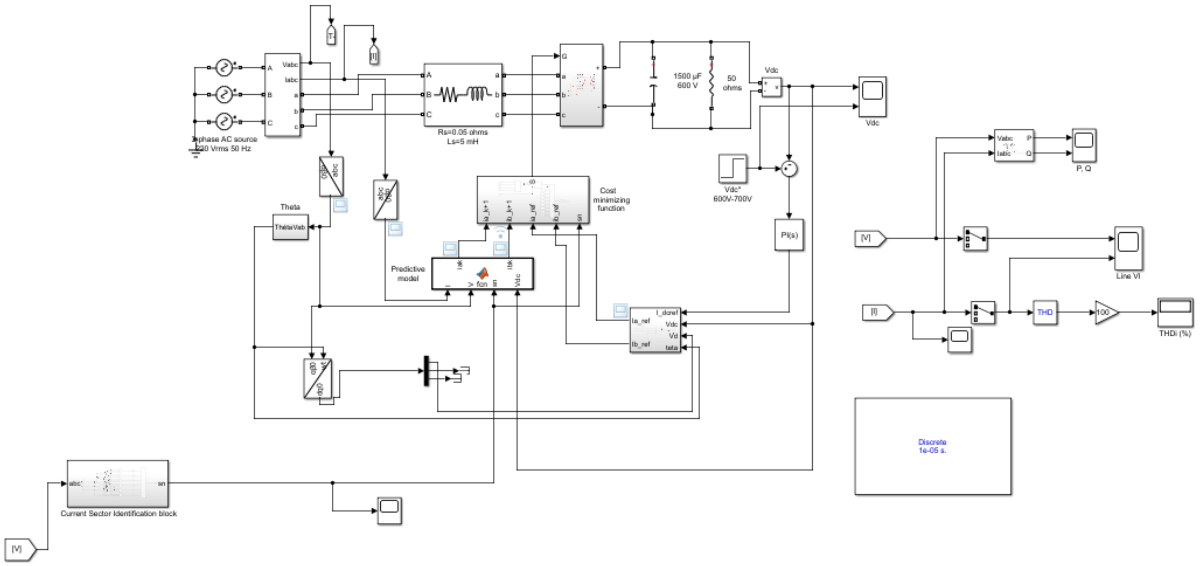

Fig.C.10 Schematic of the overall system for Vienna rectifier with FCS-MPC

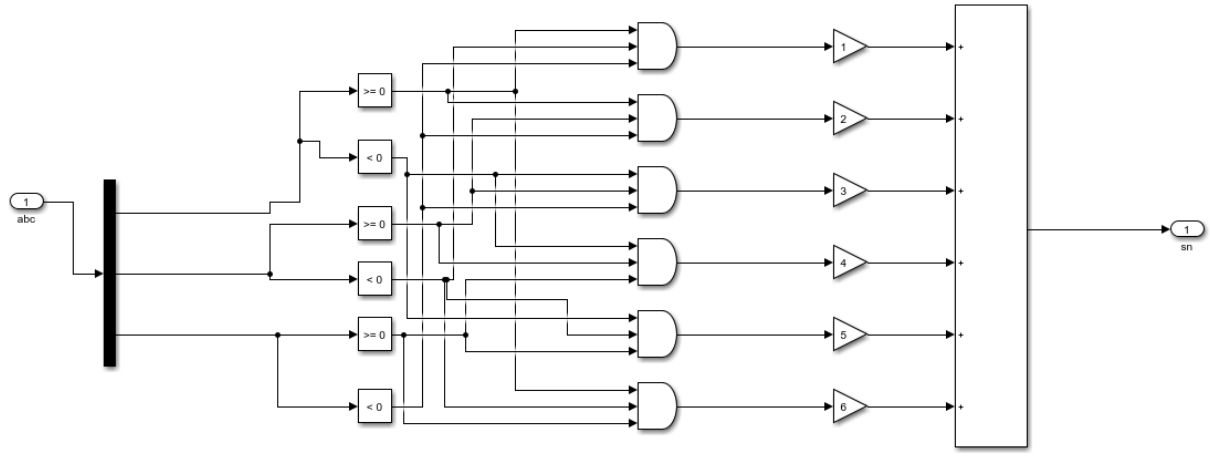

Fig.C.11 Sector Identification block

Parameter Value
Sampling frequency 100 khz
Line voltage 220 V
Grid frequency 50 Hz
Line inductance 5 mH
Line resistance 0.05 Ω
DC-side capacitor 1500 µF
Initial capacitor storage 600 V
Load resistance 50 Ω
Switching frequency 5 kHz
Hysteresis band Hp, Hq 2 W, 2 VAR

Table.C.1 Simulated network parameters

References

[1] DJABALI Sarah, AIT HAMOU ALI Melissa. (2020). Control and Power Quality Improvement of Three-Phase PWM-Rectifier. Master thesis.

[2] M. Sc. Mariusz Malinowski. (2001). Sensorless control strategies for three - phase PWM rectifier. PhD thesis. Warsaw. Poland.

[3] Hui Ma, Yunxiang Xie, Biaoguang Sun and Lingjun Mo. (2015). Modeling and Direct Power Control Method of Vienna Rectifiers Using the Sliding Mode Control Approach. Journal of Power Electronics.

[4] Gowthamraj Rajendran, Chockalingam Aravind Vaithilingam, Norhisam Misron, Kanendra Naidu & Md Rishad Ahmed. (2021). Voltage Oriented Controller Based Vienna Rectifier for Electric Vehicle Charging Stations. IEEE Access.

[5] Ali Saadon Al-Ogaili , Ishak Bin Aris , Renuga Verayiah , Agileswari Ramasamy , Marayati Marsadek , Nur Azzammudin Rahmat , Yap Hoon , Ahmed Aljanad and Ahmed N. Al-Masri. (2019). A Three-Level Universal Electric Vehicle Charger Based on Voltage-Oriented Control and Pulse-Width Modulation. Energies. vol. 12, no. 12, p. 2375,

[6] Ali R. Izadinia, Hamid R. Karshenas. (2016). Optimized Current Control of Vienna Rectifier Using Finite Control Set Model Predictive Control.

[7] Zhang, Yongchang & Peng, Yubin & Qu, Changqi. (2016). Model Predictive Control and Direct Power Control for PWM Rectifiers with Active Power Ripple Minimization. IEEE Transactions on Industry Applications.

[8] Xi, Yugeng & Li, Dewei. (2019). Predictive Control: Fundamentals and Developments.

[9] Ali Sunbul, Vijay K. Sood. (2019). Simplified SVPWM Method for the Vienna Rectifier. Department of Electrical, Computer and Software Engineering, University of Ontario Institute of Technology (UOIT). Ontario. Canada.

[10] M. Sc. Majid Hosseini Khorasgani, M. Sc. Alireza Izadinia & Hamid R. Karshenas. (2016). Finite Control Set Model Predictive Control for dc Voltage Balancing in Vienna Rectifier.

[11] Ranjan Kumar Jena. ELECTRICAL POWER QUALITY. Department of Electrical Engineering. CET. BBSR.

[12] Marketing department of Meco industries Pvt, Ltd. (2005). Harmonics – A power quality problem. Industry watch – Electrical & Electronics.

[13] Ramon Pinvol. (2015). HARMONICS: CAUSES, EFFECTES AND MINIMIZATION. Salicru white papers

[14] K.Deepa, P.Ajay Kumar, V.Sai Krishna, P.N.Koteswara Rao, Mounika.A, D.Medhini. (2017). A Study of Comparative Analysis of Different PWM Techniques. Department of Electrical and Electronics Engineering, Amrita School of Engineering Bengaluru, Amrita Vishwa Vidyapeetham, Amrita University. India.

[15] Zhenyu Yu, Arefeen Mohammed, Issa Panahi. (1997). A Review of Three PWM Techniques. Texas Instruments DSP Automotive/Industrial Control Applications Houston, TX 77477.

[16] Abid E. Mansuri. (2020). Analysis of Various PWM Techniques for Three-phase Asynchronous Motor. Sardar Vallabhbhai National Institute of Technology. India

[17] F. Benchabane, A. Titaouine, O. Bennis, K. Yahia, D. Taibi. (2012). Direct field-oriented control scheme for space vector modulated AC/DC/AC converter-fed induction motor.

[18] Ali Sunbul. (2019). Controlling the Vienna Rectifier Using a Simplified Space Vector Pulse Width Modulation Technique. Master thesis.

[19] Jin-Woo Jung. (2005). Space Vector PWM Inverter [project]. Department of Electrical and Computer Engineering. Ohio state university, United State of America.

[20] M. Hartmann, et al. (2009). Digital current controller for a 1MHz, 10kW three-phase Vienna rectifier. IEEE Trans. Power Electron.

[21] Johann W. Kolar, Franz C. Zach. (1997). A Novel Three-Phase Utility Interface Minimizing Line Current Harmonics of High-Power Telecommunications Rectifier Modules. IEEE Transactions on industrial electronics.

[22] FENG YU, XING LIU, XINSONG ZHANG & ZHIHAO ZHU. (2019). Model Predictive Virtual-Flux Control of Three-Phase Vienna Rectifier Without Voltage Sensors. IEEE Access.

[23] YAHIAOUI Juba. (2017). Design and Implementation of Vienna Rectifier Using dsPIC. Master thesis

[24] Hongli Cheng, Jing Huang. (2018). Research on SVPWM Control Strategy of Three Phase VIENNA Rectifier.

[25] Ferdinant Visser. (2011). Design and implementation of a bi-directional 3-phase converter for a 30kW range extender application. Master thesis.

[26] Nereus Fernandes, Special seminar on "Control Schemes for Three-Phase Boost Type Pulse Width Modulated Rectifier".

[27] Kasmierkowski Marian P., Blaabjerg F., Krishnan R. (2002). Control in power electronics, selected problem. Elsevier Science, United State of America.

[28] Sylvain LECHAT SANJUAN. (2010). Voltage Oriented Control of Three-Phase Boost PWM Converters Design, simulation and implementation of a 3-phase boost battery charger. Master of Science Thesis in Electric Power Engineering. Sweden.

[29] Zhang, Yongchang & Qin, & Zhengxi, & Yingchao. (2013). Comparative study of model predictive current control and voltage-oriented control for PWM rectifiers.

[30] Eskandari-Torbati, Hamid & A. khaburi, Davood. (2013). Direct Power Control of three phase PWM rectifier using Model Predictive Control and SVM switching.

[31] Zeyu Shi, Yunxiang Xie, Yingpin Wang, Hui Ma and Jienan Zhang (2018). Improved model predictive control for three-phase Vienna rectifiers. IEICE Electronics Express.

[32] Rodriguez, J. & Cortes, Patricio. (2012). Predictive Control of Power Converters and Electrical Drives.

[33] J. Rodriguez, et al. (2007). Predictive current control of a voltage source inverter. IEEE Trans. Ind. Electron.

[34] Surajit Chattopadhyay, Madhuchhanda Mitra and Smarjit Sengupta. (2011). Electric Power Quality.

[35] Ali Abdul Razzaq Altahir. (2020) Park and Clark Transformations: A Short Review.

[36] T. Thandapani, R. Karpagam and S.Paramasivam. (2015). Comparative study of VIENNA rectifier topologies. Int. J. Power Electronics, Vol. 7